“RUB-IMPACT ANALYSIS IN ROTOR DYNAMIC SYSTEMS”

A Thesis Submitted in partial fulfillment
of the requirements for the award of

Master of Technology

In

Machine Design and Analysis

By

Veluri.Gangadhar

Roll No: 209ME1184

Department of Mechanical Engineering
National Institute of Technology-Rourkela
Rourkela -769008
2011

“RUB-IMPACT ANALYSIS IN ROTOR DYNAMIC SYSTEMS”

A Thesis Submitted in partial fulfillment
of the requirements for the award of

Master of Technology

In

Machine Design and Analysis

By

Veluri.Gangadhar
Roll No: 209ME1184

Under the Guidance of

Dr. J.Srinivas

Department of Mechanical Engineering
National Institute of Technology
Rourkela
2011

NATIONAL INSTITUTE OF TECHNOLOGY
ROURKELA

CERTIFICATE

This is to certify that the thesis entitled, **"RUB-IMPACT ANALYSIS IN ROTOR DYNAMIC SYSTEMS"** by **Mr. Veluri Ganagadhar** in partial fulfillment of the requirements for the award of **Master of Technology** Degree in ***Mechanical Engineering*** with specialization in "**Machine Design & Analysis**" at the National Institute of Technology, Rourkela is an authentic work carried out by him under my supervision and guidance.

To the best of my knowledge the matter embodied in the thesis has not been submitted to any other University/ Institute for the award of any Degree or Diploma.

Date:

Dr. J. Srinivas
Dept. of Mechanical Engineering
National Institute of Technology
Rourkela-769008

ACKNOWLEDGEMENT

Successful completion of this work will never be one man's task. It requires hard work in right direction. There are many who have helped to make my experience as a student a rewarding one.

In particular, I express my gratitude and deep regards to my thesis guide **Prof. J. Srinivas,** first for his valuable guidance, constant encouragement and kind co-operation throughout period of work which has been instrumental in the success of thesis.

I also express my sincere gratitude to **Prof. R. K. Sahoo**, Head of the Department, Mechanical Engineering, for providing valuable departmental facilities.

Finally, I would like to thank my fellow post-graduate students.

Veluri Gangadhar
Roll No. 209ME1184
Department of Mechanical Engineering
National Institute of Technology
Rourkela

ABSTRACT

Considering the needs of high rotating speed and high efficiency in the modern machines, the decreasing clearance between the rotor and the stator is a necessary design. To improve the performance efficiency of these kinds of machines, the radial clearance between the rotating rotor and the stator becomes smaller and smaller. As a result, it is easier for rotor-stator rub to happen and the normal operation of machines will be affected more severely. When a rub-impact happens, the partial rub arises at first. During a complete period, the rub and impact interactions occur between the rotor and stator once or fewer times. Gradual deterioration of the partial rub will lead to the full rub and then the vibration will affect the normal operation of the machines severely. The majority of works was focused on the development of some mathematical models in order to make the rubbing phenomenon more accurately to be understood in the past few decades. Now in our work general model of a rub-impact rotor-bearing system is set up and the corresponding governing motion equations are given. The rubbing model consists of the following forces i.e., radial elastic impact and the tangential Coulomb type of friction. Through numerical calculations, rotating speeds, unbalance and stiffness values are used as control parameters to investigate their effect on the rotor-dynamic system with the help of time histories, phase plane plots, whirl orbits. Complicated motions, such as periodic, quasi-periodic even chaotic vibrations, are observed under different operating conditions. Stator flexibility effects are also studied using a modified Jeffcott rotor model .Numerical methods employed in our work are Newmark's method and Runge-Kutta method .The Graphs that have been obtained from both methods were compared Finite Element Model of the rotor dynamic system is developed with 2-noded Timoshenko beam elements. The rotary degrees of freedom are eliminated by static condensation. The Campbell diagram is obtained by accounting both gyroscopic effect and Viscous damping matrices. The Newmark time integration scheme is adopted again by incorporating the intermittent rubbing forces at the central node simulating the rigid disk stator interactions and we are trying to get the results, to compare with the obtained results. The thesis is organized as follows: Chapter-1 describes introduction to rotor dynamic problem and literature survey. Chapter-2 deals with the dynamic modeling and equations of motion of various models considered in the present work. Chapter-3 describes the results part as solution of these equations. Chapter-4 gives summary and conclusions of the work.

NOMENCLATURE

K = Non dimensional stiffness ratio

$\boldsymbol{F_n, F_t}$ = radial impact, tangential rubbing forces

$\boldsymbol{F_x, F_y}$ = rub-impacting force in the x and y directions

O = geometric center of end bearing

$\boldsymbol{O_s}$ = center of the stator

R = non dimensional radial displacement of the rotor

U = non dimensional imbalance;

X_r, X_s = non dimensional displacement of the rotorand stator in the horizontal direction ;

Y_r ,Y_s =non dimensional displacement of the rotor and stator in the vertical direction;

Ω =non dimensional rotating speed of the rotor

$\Delta \boldsymbol{X}$ =initial horizontal eccentric ratio

$\Delta \boldsymbol{Y}$ = initial vertical eccentric ratio

C = damping of the shaft

k = stiffness of the shaft

$\boldsymbol{k_c}$ = contact stiffness

r = radial displacement of the rotor

X = displacement of the rotor in the horizontal direction

y = displacement of the rotor in the vertical direction

δ = radial clearance between rotor and stator

μ = friction coefficient between rotor and stator

$\boldsymbol{\tau}$ = non dimensional time;

ω = rotating speed of the rotor

$\boldsymbol{\omega_n}$ = natural frequency of the rotor;

$\boldsymbol{\xi}_r$, $\boldsymbol{\xi}_s$ = non-dimensional damping of the Rotor and stator

CONTENTS

1. INTRODUCTION

Rotor dynamic systems often have a shaft carrying one or several disks supported on the bearing system. In industries, shaft rotating in seals or disks covered by casing often undergo metal to metal contact. Such problems are of relative importance from academic and industry point of view in view of non-linear dynamic involved in the analysis.

1.1 Rub Impact in rotors

Since the invention of the wheel, rotors have been the most commonly used part of machines and mechanisms .While fulfilling very important roles in machinery, the rotors are, at the same time, the main source of perturbation of normal operation of the machines. Rotational motion around an appropriate axis, at rated ,design –imposed, rotational speed, represents the crucially required dynamical state for rotors .The rotor rotation may be accompanied by various modes of vibrations namely lateral, torsional and axial modes .Among these modes ,the lateral modes of the rotor are of great concern .Unfortunately with the increase of the rotational speed and rotational energy, the mechanical side effects has become more and more pronounced and more dangerous for the integrity of the machine and safety of the environment. There are many factors which lead to unnecessary vibrations and important one among them is rotor unbalance. Rotor unbalance is a condition of uneven mass distribution in the radial directions at each axial section of the rotor. In an Unbalanced condition, the rotor mass centerline does not coincide with the axis of rotation. Unbalance can result from rotor material nonhomogeneity like voids, porosity, inclusions etc. Specific types of imperfections in design, fabrication and assembly can also cause unbalance. Unbalance may also occur during machine operation due to erosion or build up of deposits on the rotor, missing or loose rotor parts, or load-related and/or thermal distortion of the rotor. The unbalance may also occur due to rotor crack. The rotor unbalance acts, therefore in the lateral vibration mode, like an external exciting centrifugal force. This force leads to a malfunction in rotating machines which is nothing but rotor to stator contact. Dynamic characteristics of most rotating machines also depend on physical phenomena taking place in rotor –surrounding fluids, particularly the phenomena occurring in fluid lubricated bearings, seals, blade tip clearances, rotot/sator air gaps .Rotating vibration monitoring and diagnostics starts with implementation of basic transducers in machine systems. vibration transducers provide important information about the dynamic process taking place within the machine .The basic data acquired from the transducers is then processed in order to pull out the most important information regarding machine operation.

Radial clearance between rotor and stator in high-speed rotating machines such as generator sets, aeroengines , turbines, and compressors is of great importance. If the radial clearance

between the rotating rotor and the stator is smaller , the efficiency of these kinds of machines improves .But mass Unbalance related vibrations of the rotor draw energy from rotation to vibration, thus the overall efficiency of the rotating machines diminishes .An unbalance causes vibration and alternating or variable stress in the rotor itself and its supporting structural elements The vibration may result in in excessive wear in bearing bushings, spindles, gears etc. Stresses in the rotor and supporting structure may cause fatigue cracks , leading to a possible fatigue failure. High synchronous vibrations of the rotor may exceed available clearances and cause rubbing between rotor and stator .This rotor physical contact with a stationary element (stator) of rotating machine and the subsequent rubbing at the contact area is serious malfunction in rotating machinery that may lead to machines failure. The physical contact of the rotating rotor in operation with a stationary element involves several major physical phenomena such as friction, impacting, modification of the system stiffness etc. Friction at the contacting surfaces generates tangential force pointed in a direction which opposed to rotational speed. Friction force depends on normal force and surface properties and is the main contributor to surface wear at the rotor/stator contact location. Rubbing friction may also produce material deposition, which again, would change clearance and contacting surface conditions. As a result of the rub, the normal operations of machine is effected and generally worsened.

Heavy rubs cause impacts, chaotic motions as well as sub-synchronous and super- synchronous vibrations of the shafts. On the contrary, light partial rubs and full annular rubs cause major progress changes in the synchronous vibrations At first partial rub arises when a rub-impact happens .During a complete period once or fewer times the rub impact interactions occur between the rotor and stator .Gradual deterioration of the partial rub will lead to the full rub and then the vibration will affect the normal operation of the machines severely. Complicated nonlinear behavior is generally associated with a vibrating system of a faulty rotor. Regarding some types of faults, the vibration of system contains a very complicated phenomenon including not only the periodic motion but also the chaotic motion. Therefore to establish a reliable diagnosis system for the rotating machinery with different types of faults in the rotor systems, a detailed investigation on various forms of vibrations is of great importance.

1.2 Literature Survey

For the past two decades, majority works analyzed rub-impact analysis of rotors analytically using different mathematical models. This includes constant and accelerating rotors; rotors with or without bearing dynamics included; lumped-parameter or continuous system model or using finite element analysis. This section deals with summary of various related works collected during the work period.

Beatty [1] proposed a mathematical model for rubbing forces and a detailed response format of diagnostic data in actual cases. The model is still applied widely today. A comprehensive investigation on

the dynamic characteristics exhibited by this kind of system is necessary in order to diagnose this fault. Choyand Padovan [2] performed a very interesting theoretical investigation to observe the effects of casing stiffness, friction coefficient, imbalance load, system damping on rub force history, and the transient response of rotor orbit; but only periodic vibration was discussed. Choi and Noah [3] examined the complex dynamic behavior of a simple horizontal Jeffcott rotor with bearing clearances. Numerical results have revealed the alternating periodic. He proposed a numerical method which combined the harmonic balance method with discrete Fourier transformation and inverse discrete Fourier transformation. Their numerical results show the occurrence of super and subharmonics located in a rotor model involved a bearing clearance.

Chu and Zhang [4] performed a numerical investigation to observe periodic, quasi-periodic and chaotic motions in a rub-impact rotor system which is supported on the oil film bearings. Routes into and out of chaos were analyzed. They discussed a nonlinear vibration of the Jeffcott rotor system which includes a nonlinear rub-impact forces resulted from the eccentric rotation of rotor. They found that whenever the rub-impact occurs, three kinds of routes into the chaos will arise as the rotating speed increases. Edwards *et al*.[5] investigated the torsion effect included in a contacting rotor-stator system. They also examined the system's response regarding the torsional stiffness, and concluded that torsion has a substantial effect on system response. Shang *et al*.[6] investigated the global response characteristics of a general rotor/stator rubbing system, which takes into account the dominant factors in the process of rotor/stator rubbing, especially, the dry friction effect that is mostly neglected and provide good understanding on the coexistence of different rubbing responses observed in tests. Roques *et al*.[7] introduced a rotor–stator model of a turbo generator in order to investigate speed transients with rotor-to-stator rubbing caused by an accidental blade-off imbalance and highly nonlinear equations due to contact conditions are solved through an explicit prediction–correction time-marching procedure combined with the Lagrange multiplier approach dealing with a node-to-line contact strategy. and numerical Lu *et al*.[8] presented a method consisting of analytical and numerical techniques to solve the existence problem of rub-impact periodic motions.

Shen *et al*.[9] introduced general model of a rub-impact rotor-bearing system with initial permanent bow and through numerical calculation, rotating speeds, initial permanent bow lengths and phase angles between the mass eccentricity direction and the rotor permanent bow direction are used as control parameters to investigate their effect on the rub-impact rotor-bearing system with the help of bifurcation diagrams, Lyapunov exponents, Poincaré maps, frequency spectrums and orbit maps. Jeng *et al*.[10] presented an alternative Poincare´ section for high-order harmonic and chaotic responses of a rubbing rotor ,in this paper they introduced an alternative Poincare´ section method to analyze the dynamic behavior of a rotor in rubbing. This response integration for analyzing high-order harmonic and

chaotic responses is used to integrate the distance between state trajectory and the origin in the phase plane during a specific period. They concluded that, from simulation results, it shows that the responses of a rubbing rotor exhibit very complicated types of higher subharmonic oscillation, period. Rad *et al*.[11] made thermoelastic modeling of rotor response With shaft rub, they presented the effects of shaft rub on a rotating system's vibration response with emphasis on heat generation at the contact point. A 3D heat transfer code, coupled with a 3D vibration code, was developed to predict the dynamic response of a rotor in the time domain. It was found that friction coefficient and increasing mass unbalance amplified the rub effects while acceleration/deceleration rate reduced it.

Chu and Lu [12] found the rubbing location in a multi-disk rotor system by means of dynamic stiffness identification approach. Fulei and Zhang[13] predicted the periodic ,quasi periodic, and chaotic Vibrations of a rub impact rotor system supported on oil film bearings. Chu [14] studied about stability and non-linear responses of a rotor-bearing system with pedestal looseness Stability of the periodic solutions is analyzed by using the. Different forms of periodic, quasi-periodic and chaotic vibrations are observed Peng *et al*.[15] detected the rubbing-caused impacts for rotor–stator fault diagnosis using reassigned scalogram. In his research, the common fault of rubbing between a rotor and a stator has been modeled and studied. It is found that the more serious the rubbing, the more the number of impacts appearing in the high-frequency regions and the stronger the amplitude of these impacts With help from the reassigned scalogram they improved the readability of the results by reducing interference and enhancing the concentrations in both time and frequency domain. Hence, the occurrence time and the period of high-frequency impacts are possible to be determined. Kim and Naoh [16] conducted the bifurcation analysis for modified Jeffcott rotor with bearing clearances. He used harmonic balance technique to obtain synchronous and sub-synchronous whirling motions of a horizontal Jeffcott rotor with bearing clearances. The method utilizes an explicit Jacobian form for the iterative process.

Diken[17] worked on nonlinear vibration analysis and subharmonic whirl frequencies of the Jeffcott rotor model In this analysis, a Jeffcott rotor model is used which is a thin disk located on a flexible shaft which is simply supported at the ends. The non-linear dynamic equations of the rotor are obtained. A perturbation technique is used to obtain approximate linear equations for the non-linear equations. The non-linear equations and approximate linear equations are solved numerically and the solutions compared. The study shows that there exist two subharmonic transient vibrations caused by the non-linearity of the system itself. Kim *et al*.[18] predicted the periodic response of multi-disk rotors with bearing clearances The results reveal the interrelated roles of the bearing clearance, mass eccentricity and side force in producing dangerous subharmonics. The significant effects of the strong non-linearity of a bearing clearance are studied as related to the various system parameters. The results show that the approach developed in study is computationally superior to numerical integration methods in analyzing

multi-disk rotor systems with strong non-linearity. Patel and Darpe [19] worked on coupled bending-torsional vibration analysis of rotor with rub and crack. In this paper, modelling and vibration signature analysis of rotor with rotor–stator rub, transverse fatigue crack and unbalance is attempted. The rotor–stator interaction effects on the response of a rotor are investigated in the presence/absence of a transverse crack.

Chang-Jian and Chen [20] investigated the Chaos and bifurcation of a flexible rub-impact rotor supported by oil film bearings with nonlinear suspension The dynamic analysis of the rotor-bearing system is studied in this paper and is supported by oil film journal bearings. An observation of a nonlinearly supported model and the rub-impact between rotor and stator is needed for more precise analysis of rotor-bearing systems. Inclusive of the analysis methods of the dynamic trajectory, the power spectra, the Poincare maps, the bifurcation diagrams and the Lyapunov exponent are used to analyze the behavior of the rotor centre and bearing centre in the horizontal and vertical directions under different operating conditions. The periodic, quasi-periodic, sub-harmonic and chaotic motion are demonstrated in this study. It is concluded that the trajectory of rotor centre and bearing centre have undesirable vibrations.

Shen *et al*. [21] studied the effect of parameters on the rubbing condition of an unbalanced rotor system with initial permanent deflection. Through the analytical method, the rubbing condition was analyzed. Whether the rub would happen and when the rub would happen was well solved. The amplitude of the rotor center was calculated, and the rubbing factor was introduced to determine whether the rub would happen or not for all rotating speeds. Rubbing speeds when rub began to happen were obtained. Parameters such as the mass eccentricity, the initial permanent deflection, damping coefficients, and the phase angle between the mass eccentricity and the permanent deflection were used to analyze their effect on the rubbing condition. Pennacchi and Vania [22] analyzed rotor-to-stator rub in a large steam turbo-generator. The aim of this paper is to present an actual case history of a large turbo-generator unit that was subjected to partial arc rubs. The experimental results are shown and discussed along with the model-based diagnostic strategy employed to identify the fault severity and the location of the shaft cross-sections where the heaviest rubs occurred. Comparisons between experimental data and simulated vibrations caused by the identified fault are shown to validate the proposed methodology. Chu and Lu [23] investigated the Stiffening effect of the rotor during the rotor-to-stator rub in a rotating machine. In this paper, the dynamic model of the rubbing rotor system is established and the dynamics of the rubbing rotor is investigated. The parameter identification is used to process the vibration data obtained by numerical simulation and experimental test. The change in the transient stiffness of the rotor is analyzed and the stiffening effect of the rotor is investigated quantitatively. It is found that the change of the transient stiffness can effectively reflect the severity of the rub–impact.

Chu and Lu [24] presented an experimental set up to stimulate the rotor to stator rub of rotor system nonlinear responses and bifurcation characteristics of system are predicted using vibration wave forms, spectra, orbits and Poincare maps. Experiments with different conditions, including one and two rotor with single and multi disks are performed. Abuzaid *et al*.[25] investigated the effect of partial rotor to stator rub using both analytical and experimental methods. Light rubbing induced vibrations were shown to be characterized by harmonics at frequencies equal to 1x, 2x and 3x revolutions. The resonant frequencies were found to be increased due to stiffening effect of rubbing of rotor.

Some authors even worked on the rub impact rotor system in MEMS. Zhang and Meng [26] established Jeffcott micro-rotor system with rub –impact using classical impact theory and analyzed by modern nonlinear dynamics and bifurcation theories. It was found that the system goes through extraordinary route to chaos and alternates among periodic, quasiperiodic and chaotic motions as the system parameters change. Li *et al*.[27] proposed a novel nonlinear model of rotor/bearing/seal system for steam turbines in power plants. Musznyska model for steam forces and unsteady bearing oil film force model were applied. Runge –Kutta method was used to solve the motion equation of the system. Dynamic characteristics of rotor/bearing system were analyzed using bifurcation diagram, time histories, trajectory plots (phase diagrams), Poincare maps and frequency spectrum. Yang *et al*.[28] developed a finite element model of dual-span rotor system with rub impact at fixed limiter. System motion characteristics in different rotating speeds and rub impact rod stiffness are investigated numerically by Hilbert-Huang transforms (time-frequency analysis).

Recently, several authors have shown interest in accelerating rotor dynamics. Zapomel and Ferfecki [29] derived the equations of motion of a continuous rotor turning with variable revolutions supported over the fluid-film bearings. The Hertz theory is applied to determine the contact forces. Calculation of the hydrodynamic forces acting on the bearings is based on solving the Reynolds equation and taking cavitation into account. Lagrange equations of the second kind and the principle of virtual work are used to derive equations of motion. The Runge–Kutta method with an adaptive time step is applied for their solution. Patel and Darpe [30] in another work studied the coast-up lateral vibration response of rotor-stator rub. Rub detection at initial stage was attempted. Shift in resonance speed and the directional nature of the rub fault were observed. Potential of Hilbert–Huang transform over wavelet transform is examined. Appearance of the sub-synchronous frequencies in these transforms was suggested for early rub detection.

1.3 Objectives of the present work

In present work, general two-dimensional model of a rub-impact rotor-bearing system is employed and the corresponding governing motion equations are presented. The rubbing model consists of the following

forces: gravity, unbalance and radial elastic impact and the tangential Coulomb type of friction. The solution of equations of motion is obtained through numerical time-integration (Newmark-β) scheme, the dynamic response of this system is to be arrived and to be validated with explicit Runge-Kutta scheme. The solutions are shown in the form of time histories, phase plane plots, whirl orbits and Poincare diagrams by considering the rotating speed, unbalance and rub-impact stiffness as variables.

Periodic, quasi-periodic and chaotic vibrations are identified under different operating conditions. As a more general model, stator flexibility effect is also studied and a general formulation of finite element procedure for the single-disk rotor mounted over simply supported bearings is presented using Timoshenko beam theory. All these numerical simulations are implemented using MATLAB computer programs.

2. MATHEMATICAL MODELLING

Nonlinear dynamics of rotating system has been subject of many studies over past decades. The models presented in these studies may be classified in to two groups; in the first, rotor system is modeled as lumped masses and in second, continuous system model are used. This chapter describes modeling and formulation of equations of motion of commonly used models. The dynamic characteristics of a rotor dynamic systems system can be studied and analyzed by using simple rotor models. In these models two-degrees-of-freedoms (2-DOF) are considered and assumptions made here are not practical and do not correspond with reality, but they can allow for parametric studies and simplify the solution. These allow us to understand the effects of each parameter on rotor dynamics behaviors. They also provide many valuable physical insights into more complicated systems. Researchers most widely use a single disk centrally mounted on a uniform, flexible shaft, which is supported by two identical bearings, as illustrated in Fig. 2.1 to study and understand basic rotor-dynamics. If the bearings are infinitely stiff (rigid bearings), this model is normally referred to as the *Jeffcott Rotor*.

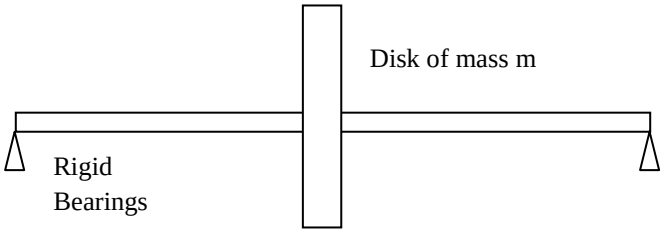

Fig 2.1 Jeffcott Rotor Model

2.1 Lumped -Parameter Models

The first model utilized in this work is based on a Jeffcott rotor described above. It is assumed that a rotor mounted on a flexible , isotropic shaft and simply supported by bearings at both ends. The weight of the rotor and shaft acts as a gravitational force which is supported by bearing force due to its stationary eccentricity. The force equilibrium of rotor in whirling with rub-impact is shown in Fig. 2.2. Here O_s is the center of the stator and O_r is center of rotor. An initial clearance of δ is provided between rotor and stator.

When rubbing between rotor and stator occurs occasionally, the elastic impact must be induced . Also, friction between both contact surfaces is assumed.

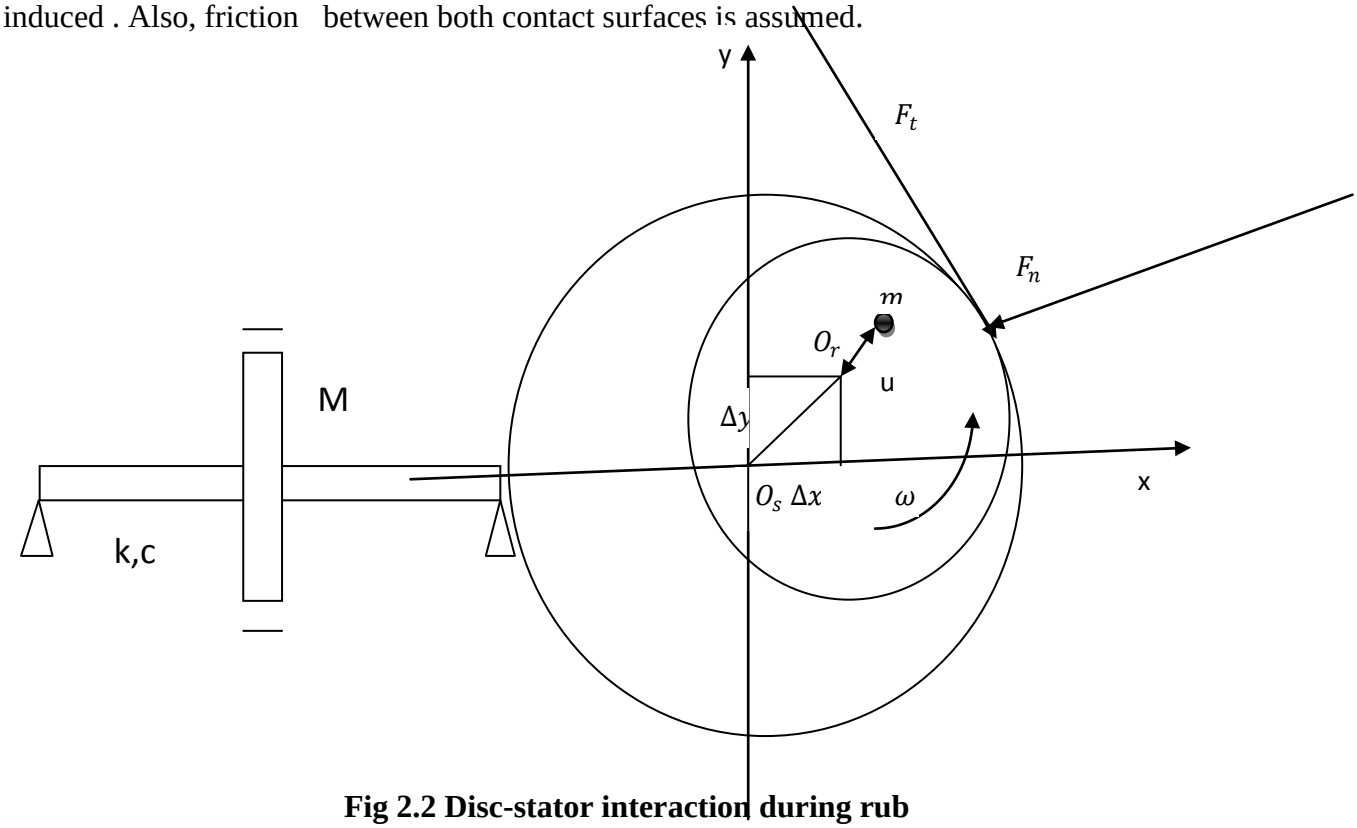

Fig 2.2 Disc-stator interaction during rub

The radial component due to impact is denoted by F_n and the tangential component due to friction is denoted by F_t which are given by

$F_n = 0$ if $(r-\delta) < 0$ (2.1)

$= k_c (r-\delta)$ if $(r-\delta) \geq 0$

and $F_t = \mu F_n$ (2.2)

where k_c is the contact stiffness of the rotor and stator; μ,is the friction coefficient, r is the radial displacement of the rotor which can be expressed as $\sqrt{(x-\Delta x)^2 + (y-\Delta y)^2}$

Here $\boldsymbol{\Delta}$x and $\boldsymbol{\Delta}$y are the initial eccentric distances in x and y directions. It indicates that whenever the radial displacement of rotor is smaller than the static clearance (δ) between rotor and stator, there will be no rub-impact; and the rub-impacting forces will be absent and the rub impact forces can be ignored in that time instance. The normal and tangential forces can be transformed in both x and y directions to give two forces F_x and F_y as follows :

$$F_x = -F_n \cos\phi + F_t \sin\phi \quad (2.3)$$

$$F_y = -F_n \sin\phi - F_t \cos\phi \quad (2.4)$$

where $\cos\phi = \frac{(x-\Delta x)}{r}$ and $\sin\phi = \frac{(y-\Delta y)}{r}$.

Substituting F_n and F_t from eqs.(2.1) and (2.2) and keeping in matrix form we get

$$\begin{bmatrix} F_x \\ F_y \end{bmatrix} = \frac{k_s(r-\delta)}{r} \begin{bmatrix} -1 & \mu \\ -\mu & -1 \end{bmatrix} \begin{bmatrix} (x-\Delta x) \\ (y-\Delta y \end{bmatrix} H(r-\delta) \tag{2.5}$$

where

$$H(r-\delta) = \begin{cases} 0, & (r-\delta) < 0 \\ 1, & (r-\delta) \geq 0 \end{cases} \tag{2.6}$$

The differential motion equations for the rotor with rub-impact can be described in x-y coordinates as

$M\ddot{x} + c\dot{x} + k\,x = mu\omega^2 \cos(\omega\, t) + F_x$ (2.7)

$M\ddot{y} + c\dot{y} + ky = mu\omega^2 \sin(\omega t) + F_y - mg$ (2.8)

where M is equivalent mass of shaft and rotor at disk , c and k are the damping and the stiffness of the shaft , respectively, ω is the rotating speed. The equations of motion were non- dimensionalized for convenience. The following dimensionless variables and parameters are selected :

$X=x/\delta$, $Y=y/\delta$, $\omega_n=\sqrt{\frac{k}{M}}$, $\Omega=\omega/\omega_n$, $T=\omega_n t$, $\xi=c/2\sqrt{kM}$, $U=mu/M\delta$, $K=k/k_s$ $R=r/\delta$

Equations (2.7) and (2.8) can be simplified as follows:

Substituting $x=X\delta$ in eq.(2.7) it becomes

$$M\delta\ddot{X} + c\delta\dot{X} + k\delta X = mu\Omega^2\omega_n^2 \cos(\Omega\omega_n\, t) + F_x \tag{2.9}$$

Dividing the last equation with $M\delta$

$$\ddot{X} + \frac{c}{M}\dot{X} + \frac{k}{M}X = \frac{mu}{M\delta}\Omega^2\omega_n^2 \cos(\Omega\omega_n\, t) + \frac{F_x}{M\delta} \tag{2.10}$$

As $\frac{c}{M}=2\xi\omega_n, \frac{k}{M} = \omega_n^2$ we can write eq (2.10) as is modified as:

$$\ddot{X} + 2\xi\omega_n\dot{X} + \omega_n^2 X = U\Omega^2\omega_n^2 \cos(\Omega\omega_n\, t) + \frac{F_x}{M\delta} \tag{2.11}$$

Now

$$\dot{X} = \frac{dX}{dt} = \frac{d}{dt}(X) = \frac{dX}{d\tau} \times \frac{d\tau}{dt}$$

$$\Rightarrow \qquad \dot{X} = X'\omega_n \text{ , where } X' = \frac{dX}{d\tau}$$

Similarly $\ddot{X} = \frac{d}{dt}(\dot{X})$

$$= \frac{d}{dt}(X'\omega_n)$$

$$= \frac{dX'}{d\tau} \times \frac{d\tau}{dt} \times \omega_n$$

$$= X'' \times \omega_n^2$$

$$= X''\omega_n^2$$

Therefore subsituting $\dot{X} = X'\omega_n$ and $\ddot{X} = X''\omega_n^2$ in eq (2.11), we get

$$\omega_n^2 X'' + 2\xi\omega_n^2 X' + \omega_n^2 X = U\Omega^2\omega_n^2 \cos(\Omega\,\tau) + \frac{F_x}{M\delta} \qquad (2.12)$$

Finally dividing the above equation with ω_n^2 , then

$$X'' + 2\xi X' + X = U\Omega^2 \cos(\Omega\tau) + \frac{F_x}{M\delta\omega_n^2} \qquad (2.13)$$

Since $M\times \omega_n^2 = k$, $\frac{F_x}{M\delta\omega_n^2} = \frac{F_x}{k\delta}$, substituting F_x from matrix eq (2.5),we can write

$\frac{F_x}{M\delta\omega_n^2}$ in eq (2.13) as :

$$\frac{F_x}{M\delta\omega_n^2} = \frac{k_s}{k} \times \frac{(r-\delta)}{r} \times \frac{[-1(x-\Delta x)+\mu(y-\Delta y]}{\delta} \times H(r-\delta) \qquad (2.14)$$

Also as $K=k/k_s$, $R=r/\delta$, $X=x/\delta$, $Y=y/\delta$, we get finally

$$\frac{F_x}{M\delta\omega_n^2} = -\frac{1}{K} \times \left(1 - \frac{1}{R}\right)[(X-\Delta X) - \mu(Y-\Delta Y)]H(R-1) \qquad (2.15)$$

Now subsituting eq.(2.15) in eq (2.13) final equation becomes

$$X'' + 2\xi X' + X = U\Omega^2 \cos(\Omega\omega_n\, t) - \frac{1}{K} \times \left(1 - \frac{1}{R}\right)[(X-\Delta X) - \mu(Y-\Delta Y)]H(R-1) \qquad (2.16)$$

where $H(R-1) = \begin{cases} 0, & (R-1) < 0 \\ 1, & (R-1) \geq 0 \end{cases}$ and the prime ie., X' indicates the time derivative with respect to τ. Similarly we can obtain in y-direction as follows:

$$Y'' + 2\xi Y' + Y = U\Omega^2 \sin(\Omega\omega_n t) - \frac{1}{K} \times \left(1 - \frac{1}{R}\right)[\mu(X - \Delta X) + (Y + \Delta Y)]H(R-1)\frac{g}{\omega_r^2 \delta} \quad (2.17)$$

If no rubbing occurs (R<1), the governing equations of motion can be written as

$$X'' + 2\xi X' + X = U\Omega^2 \cos(\Omega\omega_n t)$$

$$Y'' + 2\xi Y' + Y = U\Omega^2 \sin(\Omega\omega_n t) \quad (2.18)$$

Above approach is adopted from one of the latest article [10]. This is simplest model and it is clear that partial rubs are possible depending on the clearance and radial displacement of the rotor values, choosen in the problem.

2.1.1.Stator stiffness considerations

As shown in Fig 2.3 when the stator (casing) has a considerable stiffness its rub impact effect with stator slightly alters .A part from all variables described in above model, now the stator mass (m_s and k_s) comes in to picture. The rotor (disc) parameters are denoted with suffix 'r'.as seen in side view (Fig 2.3) ,it is assumed that origin of reference coordinate system is away from moving stator center O_s.

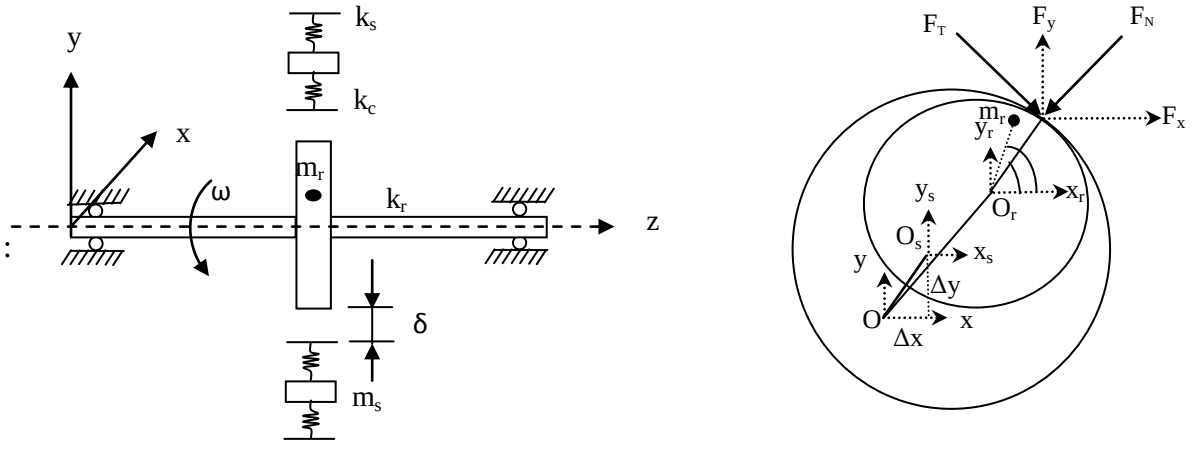

Fig 2.3 Rotor model when stator stiffness is considered

Now following the similar approach, we can write equations of motion for rotor as follows

$$m_r\ddot{x}_r + c_r\dot{x}_r + k_r x_r = m_r e\omega^2 \cos(\omega t) + F_x$$

$$m_r\ddot{y}_r + c_r\dot{y}_r + k_r y_r = m_r e\omega^2 \sin(\omega t) + F_y - m_r g \quad (2.19)$$

Equations of motion for stator are

$$m_s\ddot{x}_s + c_s\dot{x}_s + k_s x_s = -F_x$$
$$m_s\ddot{y}_s + c_s\dot{y}_s + k_s y_s = -F_y \quad (2.20)$$

where e or u is the mass eccentricity and c_r, c_s represent the damping coefficients of shaft and stator system respectively. The two intermittent forces F_x and F_y can be written as:

$$F_x = -F_n \cos\emptyset + F_t \sin\emptyset$$
$$F_y = -F_n \sin\emptyset - F_t \cos\emptyset \quad (2.21)$$

Where

$$\cos\emptyset = \frac{x_r - x_s}{|r_r - r_s|} \qquad \sin\emptyset = \frac{y_r - y_s}{|r_r - r_s|} \quad (2.22)$$

Rub and tangential forces:

It is assumed that there is an initial clearance of δ between rotor and stator and the radial force from impact is elastic. When the rubbing happens, the radial impacts force F_N and the tangential rub force F_T can be written as:

$F_n = 0$ if $|r_r - r_s| < \delta$

$= k_c(|r_r - r_s| - \delta)$ if $|r_r - r_s| \geq \delta \quad (2.23)$

$F_t = \mu F_n$ where k_c is a rub impact stiffness and $|r_r - r_s| = \sqrt{(x_r - x_s)^2 + (y_r - y_s)^2}$ is radial displacement of the rotor with respect to stator.

Now the above equations of motion of rotor and stator are non dimensionalised using following dimensionless variables $X_r = \frac{x_r}{\delta}$,$Y_r = \frac{y_r}{\delta}$, $X_s = \frac{x_s}{\delta}$, $Y_s = \frac{y_s}{\delta}$,$\omega_r = \sqrt{\frac{k_r}{m_r}}$, $\omega_s = \sqrt{\frac{k_s}{m_s}}$,$\Delta = \frac{\delta}{e}$,

$$\xi_r = \frac{c_r}{\sqrt{k_r m_r}}, \xi_s = \frac{c_s}{\sqrt{k_s m_s}}, r_1 = \frac{\omega}{\omega_r}, r_2 = \frac{\omega_s}{\omega_r}, M_{sr} = \frac{m_s}{m_r}, \alpha = \frac{k_c}{k_r}\tau = \omega_r t \quad (2.24)$$

The final non-dimensional equations are:

$$X_r'' + 2\xi_r X_r' + X_r = \frac{r_1^2}{\Delta}\cos(r_1\tau) + \frac{F_x}{m_r\omega_r^2\delta}$$
$$Y_r'' + 2\xi_r Y_r' + Y_r = \frac{r_1^2}{\Delta}\sin(r_1\tau) + \frac{F_y}{m_r\omega_r^2\delta} - \frac{g}{\delta\omega_r^2}$$
$$X_s'' + 2\xi_s r_2 X_s' + r_2^2 X_s = -\frac{F_x}{m_r\omega_r^2\delta}$$
$$Y_s'' + 2\xi_s r_2 Y_s' + r_2^2 Y_s = -\frac{F_x}{m_r\omega_r^2\delta} \quad (2.25)$$

2.2 Finite element model

The Timoshenko beam incorporates two refinements over the Bernoulli-Euler model:

1. For both statics and dynamics: plane sections remain plane but not necessarily normal to the deflected midsurface. This assumption allows the averaged shear distortion to be included in both strain and kinetic energies.

2. In dynamics: the rotary inertia is included in the kinetic energy.

The finite model of rotor bearing system is established as shown in Fig 2.4 below

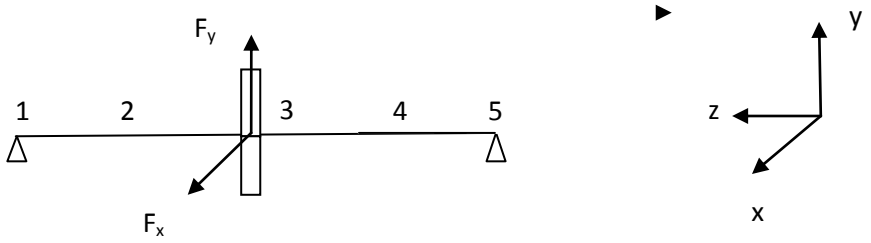

Fig 2.4 FE Model of Rotor

There are four shaft elements and five nodes all together. The Disk mass acts at node 3 as a concentrated mass. Nodes 1and 5 are rigid bearing points. Nodes 2 and 4 are at points one quarter and three quarter of length of rotor. The kinetic and potiential energy of the shaft is written as

$$T_e = \int_0^{lo} \frac{1}{2}\rho\{A(\dot{x}^2 + \dot{y}^2) + I_p[\omega^2 + \omega(\dot{\theta}_x\theta_y - \dot{\theta}_y\theta_x)]\}ds \quad (2.26)$$

$$U_e = \int_0^l \left\{EI\left[\left(\theta_x'\right)^2 + \left(\theta_y'\right)^2\right] + KGA\left[\left(\theta_y - x'\right)^2 + \left(\theta_x - y'\right)^2\right]\right\}\text{ds} \quad (2.27)$$

Work done by mass eccentricity of disk :

$$W_d = m_d e\omega^2(x\cos\omega t + y\sin\omega t) \quad (2.28)$$

The element stiffness and mass matrices are obtained by using Langranges equations. The size of the element matrices are 8×8 and the corresponding nodal degrees of freedom are x,y, θ_x, θ_y. The overall equations of motion are written as follows:

$$[M^e]\{\ddot{q}\} - \omega[G^e]\{\dot{q}\} + [C^e]\{\dot{q}\} + [K^e]\{q\} = \{f(t)\} \quad (2.29)$$

where q= $\left[x_1\ y_1\ \theta_{x_1}\ \theta_{y_1}\ x_2\ y_2\ \theta_{x_2}\ \theta_{y_2}\right]^T$

The matrices are assembled and static condensation is applied to eliminate θ_x and θ_y degrees of freedom. The force vector contains non –zero forces only at the translation degrees corresponding to node 3.

Where

ρ: density of shaft material,

A: cross-section of shaft,

I_p: Polar moment of inertia of shaft (m^4),

k: shear factor=0.65

G: shear modulus, E: Elastic Modulus

ω: shaft speed in rad/s

The element matrices as given by Nelson [1980] are presented below. Here $\frac{r}{l}$ is radius to element length ratio

$$\left[M\right]^e = \rho Al \begin{bmatrix} A_z & 0 & 0 & C_z & B_z & 0 & 0 & -D_z \\ 0 & A_y & -C_y & 0 & 0 & B_y & D_y & 0 \\ 0 & -C_y & E_y & 0 & 0 & -D_y & F_y & 0 \\ C_z & 0 & 0 & E_z & D_z & 0 & 0 & F_z \\ B_z & 0 & 0 & D_z & A_z & 0 & 0 & -C_y \\ 0 & B_y & -D_y & 0 & 0 & A_y & C_z & 0 \\ 0 & D_y & F_y & 0 & 0 & C_z & E_y & 0 \\ -D_z & 0 & 0 & F_z & -C_y & 0 & 0 & E_z \end{bmatrix} \tag{2.30}$$

$$\left[K\right]^e = \begin{bmatrix} a_z & 0 & 0 & c_z & b_z & 0 & 0 & c_z \\ 0 & a_y & d_y & 0 & 0 & b_y & d_y & 0 \\ 0 & d_y & e_y & 0 & 0 & c_y & f_y & 0 \\ c_z & 0 & 0 & e_z & d_z & 0 & 0 & f_z \\ b_z & 0 & 0 & d_z & a_z & 0 & 0 & d_y \\ 0 & b_y & c_y & 0 & 0 & a_y & c_z & 0 \\ 0 & d_y & f_y & 0 & 0 & c_z & e_y & 0 \\ c_z & 0 & 0 & f_z & d_y & 0 & 0 & e_z \end{bmatrix} \tag{2.31}$$

$$[G]^e = -2\rho Al \begin{bmatrix} 0 & g & h & 0 & 0 & -g & h & 0 \\ -g & 0 & 0 & h & g & 0 & 0 & h \\ -h & 0 & 0 & i & h & 0 & 0 & j \\ 0 & -h & -i & 0 & 0 & h & -j & 0 \\ 0 & -g & -h & 0 & 0 & g & -h & 0 \\ g & 0 & 0 & -h & -g & 0 & 0 & -h \\ -h & 0 & 0 & j & h & 0 & 0 & i \\ 0 & -h & -j & 0 & 0 & h & -i & 0 \end{bmatrix} \quad (2.32)$$

Where the constants are given by:

$A_z=A_y=\frac{\frac{13}{35}+\frac{7}{10}\varphi+\frac{1}{3}\varphi^2+\frac{3}{10}\left(\frac{r}{l}\right)^2}{(1+\varphi)^2}$ $B_z=B_y=\frac{\left(\frac{9}{70}+\frac{3}{10}\varphi+\frac{1}{6}\varphi^2\right)-\frac{3}{10}\left(\frac{r}{l}\right)^2}{(1+\varphi)^2}$

$C_z=C_y=\frac{\left[\frac{11}{210}+\frac{11}{120}\varphi+\frac{1}{24}\varphi^2+\left(\frac{1}{40}-\frac{1}{8}\varphi\right)\left(\frac{r}{l}\right)^2\right]l}{(1+\varphi)^2}$ $D_z=D_y=\frac{\left[\frac{13}{420}+\frac{3}{40}\varphi+\frac{1}{24}\varphi^2-\left(\frac{1}{40}-\frac{1}{8}\varphi\right)\left(\frac{r}{l}\right)^2\right]}{(1+\varphi)^2}$

$E_z=E_y=\frac{\left[\frac{1}{105}+\frac{1}{60}\varphi+\frac{1}{120}\varphi^2+\left(\frac{1}{30}+\frac{1}{24}\varphi+\frac{1}{12}\varphi^2\right)\left(\frac{r}{l}\right)^2\right]l^2}{(1+\varphi)^2}$ $F_z=F_y=-\frac{\left[\frac{1}{140}+\frac{1}{60}\varphi+\frac{1}{120}\varphi^2+\left(\frac{1}{120}+\frac{1}{24}\varphi-\frac{1}{24}\varphi^2\right)\left(\frac{r}{l}\right)^2\right]l^2}{(1+\varphi)^2}$

$a_z=a_y=-\frac{12EI}{l^3(1+\varphi)}$ $b_z=b_y=-\frac{12EI}{l^3(1+\varphi)}$ $c_z=c_y=\frac{6EI}{l^2(1+\varphi)}$ $d_z=d_y=-\frac{6EI}{l^2(1+\varphi)}$

$e_z=e_y=\frac{(4+\varphi)EI}{l(1+\varphi)}$

$f_z=f_y=4\times\frac{(2-\varphi)EI}{l(1+\varphi)}$

$g=4\times\frac{\left(\frac{3}{10}\right)r^2}{l^2(1+\varphi)^2}$

$h=-4\times\frac{\left(\frac{1}{40}-\frac{1}{8}\varphi\right)r^2}{l(1+\varphi)^2}$

$i=-4\times\frac{\left(\frac{1}{30}+\frac{1}{24}\varphi-\frac{1}{12}\varphi^2\right)r^2}{(1+\varphi)^2}$

$j=-4\times\frac{\left(\frac{1}{120}+\frac{1}{24}\varphi-\frac{1}{24}\varphi^2\right)r^2}{(1+\varphi)^2}$ (2.33)

Static condensation scheme is employed in this work to eliminate the angular degrees of freedom. Here θ_x ,θ_y degrees are eliminated and are called secondary degrees. The following equations are employed to get reduced matrices :

$$[K_r]=[K_{pp}]+[K_{ps}][T] \tag{2.34}$$

$$[M_r] = [M_{pp}] + [M_{ps}][T] + [T']][M_{sp}] + [T']][M_{ss}][T] \tag{2.35}$$

Where $[T] = -[K_{ss}]^{-1}[K_{sp}]$ and $[K] = \begin{bmatrix} K_{pp} & K_{ps} \\ K_{sp} & K_{ss} \end{bmatrix}$ (2.36)

2.3 Numerical integration techniques

There are many integration techniques to solve differential equations like M$\ddot{X}$+KX=F and two among them we employed are described below:

2.3.1 Newmark's Method

This integeration method is based on the assumption that the acceleration varies linearly between two instances of time.The resulting expressions for the velocity and displacement vectors for a multi –degree-of-freedom of system is written as

$$\dot{X}_{t+\Delta t} = \dot{X}_t + [(1-\partial)\ddot{X}_t + \partial\ddot{X}_{t+\Delta t}]\Delta t \tag{2.37}$$

$$X_{t+\Delta t} = X_t + \dot{X}_t\Delta t + \left[\left(\frac{1}{2}-\alpha\right)\ddot{X}_t + \alpha\ddot{X}_{t+\Delta t}\right] \tag{2.38}$$

Where α and ∂ are the parameters used to obtain integeration stability .Generally $\partial \geq 0.5$ and $\alpha \geq 0.25(0.25+\partial)^2$. $\ddot{X}_{t+\Delta t}$ and $\dot{X}_{t+\Delta t}$ are obtained in terms of $X_t, \dot{X}_t, \ddot{X}_t, X_{t+\Delta t}$.Then they are substituted in to the equation

$$[M]\,\ddot{X}_{t+\Delta t} + [C]\,\dot{X}_{t+\Delta t} + [K]\,X_{t+\Delta t} = F_{t+\Delta t} \tag{2.39}$$

Steps are summarized as follows

At time t=0

i) Form [K],[M] and [C]

ii)With the values of of $\{X_0\}$ and $\{\dot{X}_0\}$,compute $\ddot{X}_0$

iii)Choosing $\Delta t, \partial, \alpha$ such that $\partial = 0.5$ and $\alpha = 0.25(0.25+\partial)^2$ compute the following constraints

$a_1 = \frac{1}{\alpha\Delta t^2}$,$a_2 = \frac{\partial}{\alpha\Delta t}$,$a_3 = \frac{1}{\alpha\Delta t}$, $a_4 = \frac{1}{2\alpha} - 1$,$a_5 = \left(\frac{\partial}{\alpha} - 1\right)$,$a_6 = \frac{\Delta t}{2}\left(\frac{\partial}{\alpha} - 2\right)$,

$a_7 = \Delta t(1-\partial)$, $a_8 = \partial\Delta t$

iv)Form effective stiffness matrix

$$[\hat{K}] = [K] + a_1[M] + a_2[C]$$

For each time step :

i)calculate the effective load at time $(t + \Delta t)$

$$\hat{F}_{t+\Delta t}=F_t + [M]\left(a_1 X_t + a_3 \dot{X}_t + a_4 \ddot{X}_t\right) + [C](a_2 X_t + a_5 \dot{X}_t + a_6 \ddot{X}_t) \quad (2.40)$$

ii)Solve for $X_{t+\Delta t}$ from the equation ,$[\widehat{K}]X_{t+\Delta t}=\hat{F}_{t+\Delta t}$

iii)Calculate accelerations and velocities at time $(t + \Delta t)$:

$$\ddot{X}_{t+\Delta t} =a_1(X_{t+\Delta t} - X_t) - a_3 \dot{X}_t - a_4 \ddot{X}_t \quad (2.41)$$

$$\dot{X}_{t+\Delta t} = \dot{X}_t + a_7 \ddot{X}_t + a_8 \ddot{X}_{t+\Delta t} \quad (2.42)$$

2.32 Runge Kutta Method

It is an explicit integeration technique .In this method the approximate formula used for obtaining X_{i-1} from X_i is made to coincide with the Taylor's series expansion of X_i and X_{i+1} up to the terms of order Δt^n.The taylor series expansion of *X(t)* at *X(t+*Δt*)* is given by

$$X(t+\Delta t)= X(t)+\dot{X}\Delta t+\ddot{X}\frac{\Delta t^2}{1!}+\dddot{X}\frac{\Delta t^3}{3!} \quad (2.43)$$

Runge kutta method does not require explicit derivatives beyond the first.For solution of second order differential, it can be reduced to two first order equations as follows:

$$\ddot{X} =\dot{y}=\frac{1}{M}[F(t)-C\dot{X} - KX]$$

$$=M^{-1}[F(t))-C\dot{X} - KX] \quad (2.44)$$

By treating the the displacements as well as velocities as unknowns, a new vector X_1 is defined as

$$X_1=\begin{Bmatrix} X \\ \dot{X} \end{Bmatrix}$$

So that $\dot{X}_1 = \begin{Bmatrix} \dot{X} \\ [\mathrm{M}]^{-1}\left(\mathrm{F} - [C]\dot{X} - [K]X\right) \end{Bmatrix}$ (2.45)

This can be rearranged to obtain $\dot{X}_1 = \begin{bmatrix} [0] & [I] \\ -M^{-1}K & -M^{-1}C \end{bmatrix}\begin{Bmatrix} X \\ \dot{X} \end{Bmatrix}+\begin{Bmatrix} 0 \\ M^{-1}F(t) \end{Bmatrix}$ (2.46)

Thus $\dot{X}_1(t) = f(X_1, t) = [AX_1 + F(t)]$

To evaluate X_1 at different grid points t_i ,fourth order –Runge Kutta formula is used

That is $X_i\,(i+1) =X_i(i) + \frac{1}{6}[\mathrm{K}_1+2\mathrm{K}_2+2\mathrm{K}_3+\mathrm{K}_4]$ (2.47)

Where $K_1= h.\, f[X_1(i), t_i]$

$$K_2=h.\, f\left[\left(X_1(i) + \frac{K_1}{2}\right), \left(t_i + \frac{h}{2}\right)\right]$$

$$K_3 = h.\, f\left[\left(X_1(i) + \frac{K_2}{2}\right), \left(t_i + \frac{h}{2}\right)\right]$$

$$K_4 = h.\, f\left[(X_1(i) + K_3), t_{i+1}\right] \quad (2.48)$$

2.4 Tools for predicting Chaotic Vibrations

Chaos is a state of instability in which system becomes fully aperiodic and has a strange attractor. Various tools to predict chaos are

1. Phase Plane Plots
2. Frequency spectrums
3. Poincare Maps
4. Lyapunov Exponent

Phase Plane Plots: Phase trajectories are used for distinguishing periodic from non periodic and quasiperiodic motions Chaotic motions looks complicated in the phase plane .However so do other type of motions

Frequency spectrum: The spectrum associated with an arbitrary sate variable is a useful tool for distinguishing between periodic and non periodic motions. In frequency spectrum chaotic motion appears as brand band noise in the spectrum

Poincare Maps: For systems subjected to external periodic force the Poincare map is usually obtained for every time period. If the map consists of finite number of points then it indicates periodic motion and if it shows points making a curve it's a quasi periodic motion and if there are infinite number of points it shows chaotic motion

Lyapunov Exponent:Lyapunov exponent essentially measure the average rates of convergence or divergence of nearby orbits in phase space. A positive Lyapunov exponent indicates chaotic motion. Generally the largest Lyapunov exponent is only used in the analysis.

In present work, phase plane plots and Poincare maps are employed to conclude whether the system be in periodic, quasiperiodic or chaotic.

3 RESULTS AND DISCUSSION

In order to understand the dynamic instability of this rotor, following plots are constructed:
time-histories, whirl orbits, phase-diagrams and Poincare maps.

3.1 Geometric and Material data

Following geometric parameters are employed in present work for the three cases under consideration.

1.Simple model with rigid rotor (Jeng *et al*.[10])

Input Data

Parameters which are constant	$\Delta X = 0.3, \Delta Y = 0.92, \mu = 0.2, K = 0.017, \xi = 0.5$
Parameters which are varied	Unbalance(U),speedratio(Ω)
Initial conditions	Zero displacement amd velocity

2 Stator flexibility Model: (Shang et al. [6])

Input Data

Parameters and their values	M_{sr} =0.2, α=2, Δ=2, ξ_r=0.4 and ξ_s=0.4
Parameters which are varied	r_1 and r_2
Initial displacement conditions	$x_r(0)=0$, $y_r(0)=0$,$x_s(0)=1\times10^{-5}$mm, $y_s(0)=1\times10^{-5}$mm and all initial velocities are taken as zero

3 Finite Element Model Data(Li et al.[27])

Input Data

Material Properities	E=197 GPa, μ=0.3, k=0.75, density ρ=7810 kg/m^3
Dimesions of rotor	Length of shaft=1m, dia of disk=0.3m, dia of shaft=0.005m. thickness of disk=0.001m
Parameters which are varied	Speed,clearance

3.2 Results of various Models

Fig 3.1 shows the time history graph for $\Omega = 1.5$. It indicates the amplitude of the rotor in x direction. Here in this figure X-axis is nondimesional time and Y- axis is non dimensional amplitude$\frac{X}{\delta}$ amplitude of the rotor. From this figure we can observe the maximum amplitude of the rotor

is 0.18 in X-direction and it can also be observed that the amplitude of the rotor after each time period is constant.

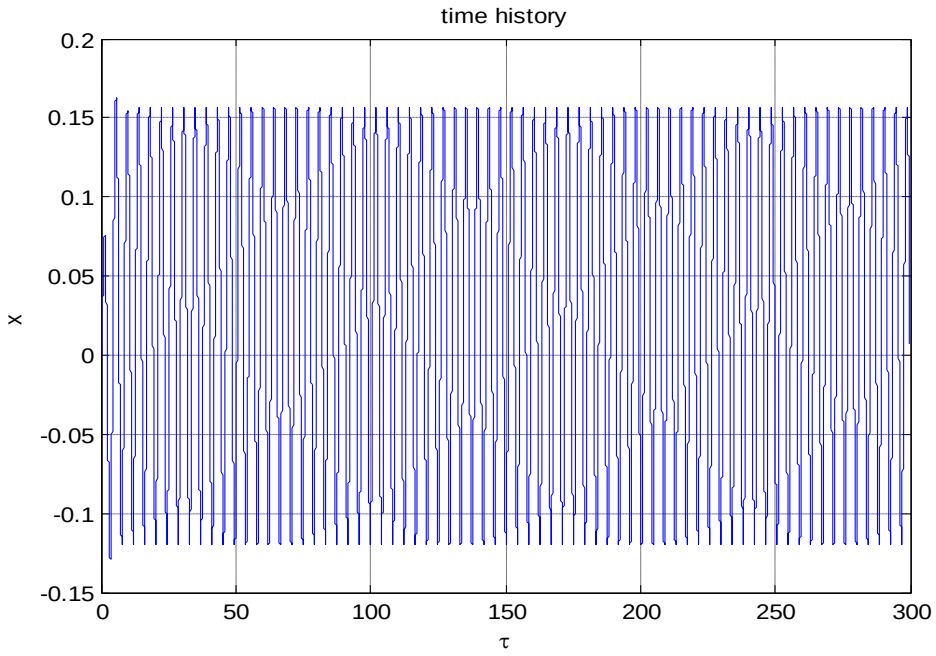

Fig 3.1 Time History diagram at disk

Fig 3.2 also represents the time history plot of the rotor system but in Y direction. The maximum amplitude of the rotor is approximately 0.19and amplitude of the rotor is observed to be constant at each time period.

PHASE PLANE PLOTS

Fig 3.3 and Fig 3.4 are phase diagrams which are the plots between the non dimensional amplitude of the rotor and its derivative in X and Ydirections respectively. As there two closed loops which are not complicated the rotor system is executing periodic motion. Fig 3.5 is a whirl orbit curve which indicates the path in which rotor travelled .It is the plot between amplitudes in X and Y direction .As the curve is simple it can be concluded that the rotor is exhibiting periodic motion

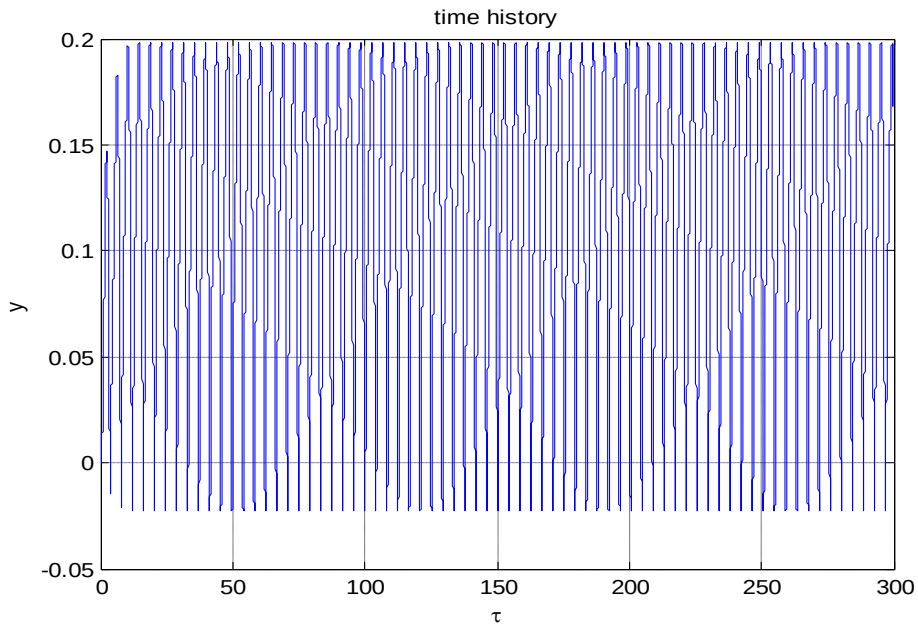

Fig 3.2 Time History

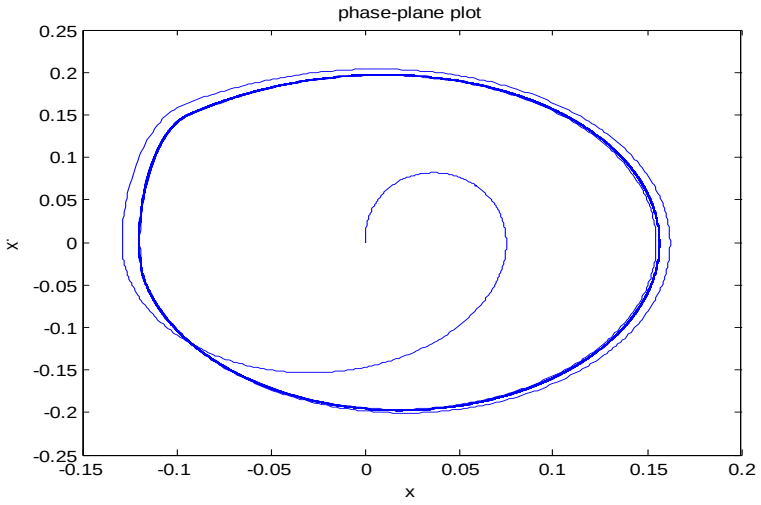

Fig 3.3 Phase plane plot

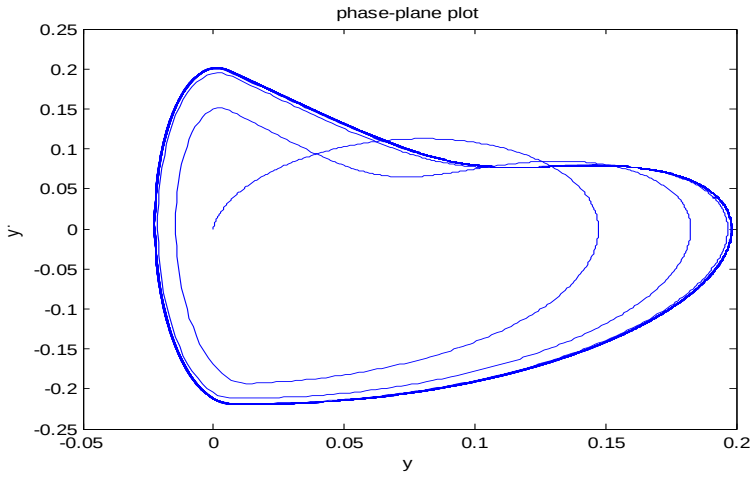

Fig 3.4 Phase plane plot

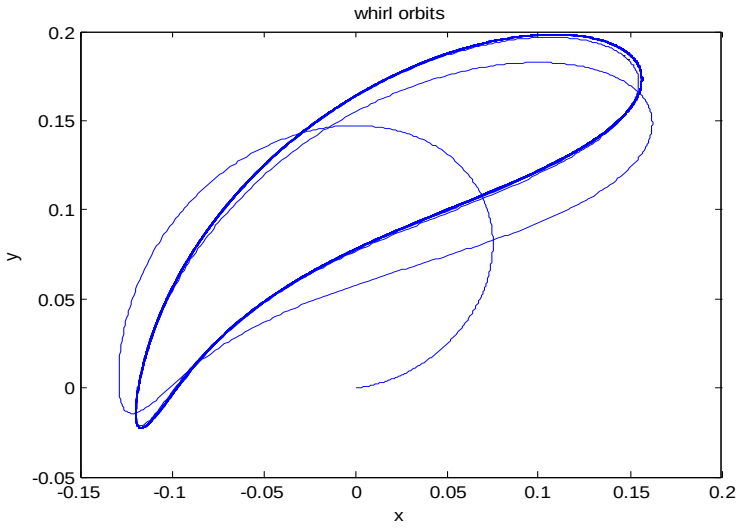

Fig 3.5 Whirl Orbit

Fig 3.6 is a Poincare map which is a plot between the amplitude and its derivative for every time period. As Poincare map is indicating four points the system is in periodic state

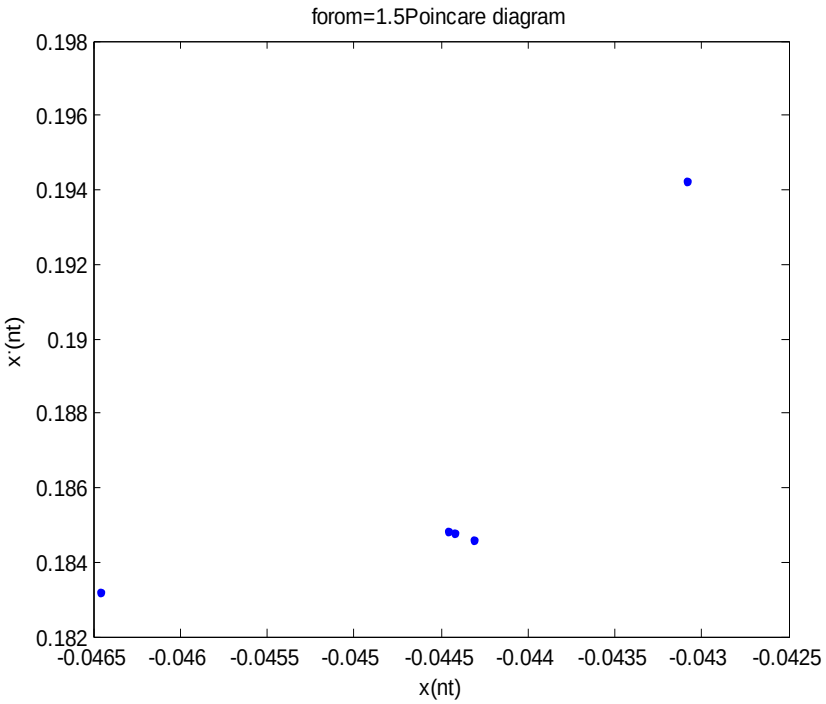

Fig 3.6 Poincare map

Figures 3.7 and 3.8 are the plots between non dimensional time and amplitude for $\Omega = 6$ Here for these conditions maximum amplitude is approximately 0.15 and also for every time period amplitude is varying

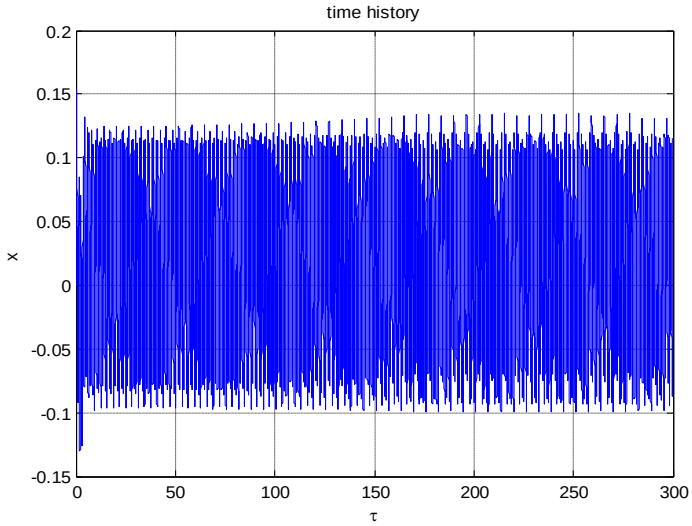

Fig 3.7 Time History

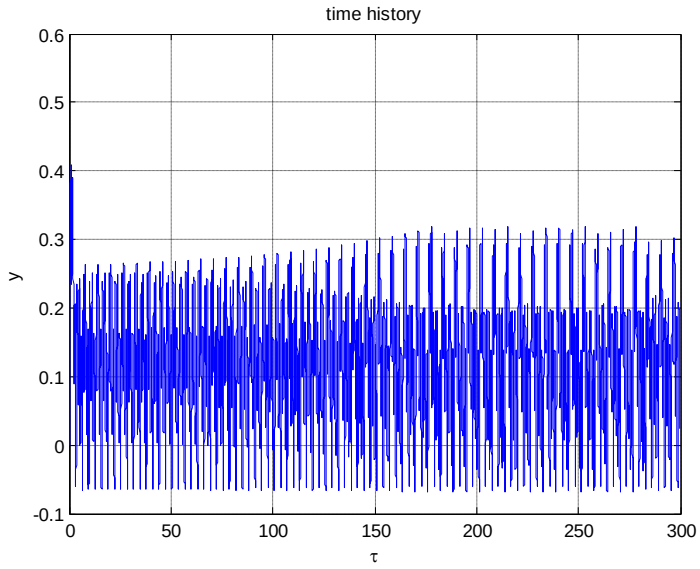

Fig 3.8 Time History

Fig 3.9 and 3.10 are phase plane plots which are nothing but plots between Nondimensional amplitude and its derivative. However as these curves don't posses single centre and are complicated. Hence the system would in chaotic sate

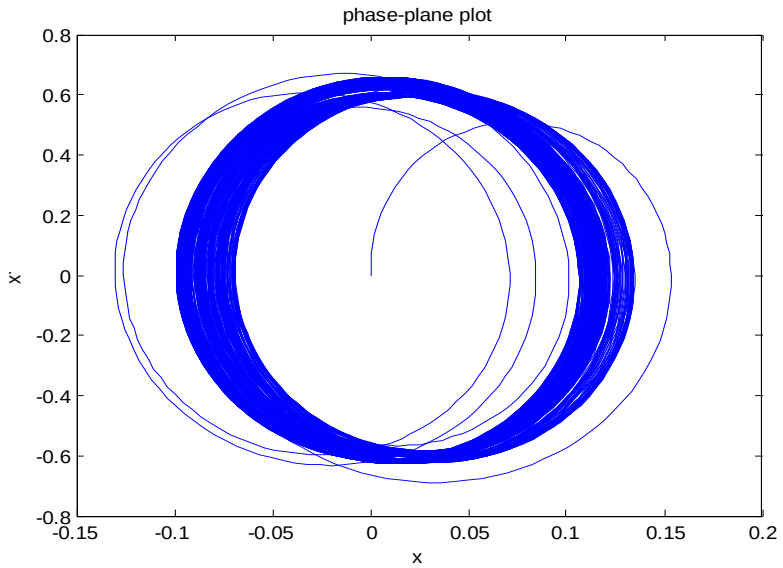

Fig 3.9 Phase Plane Plot

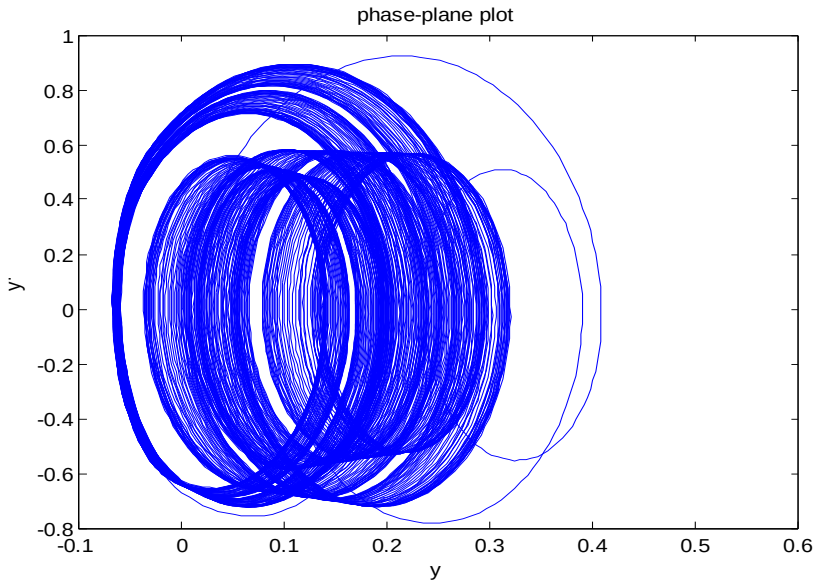

Fig 3.10 Phase Plane plot

Fig 3.11 is whirl orbit shows the complicated motion of the rotor for $\Omega = 6$

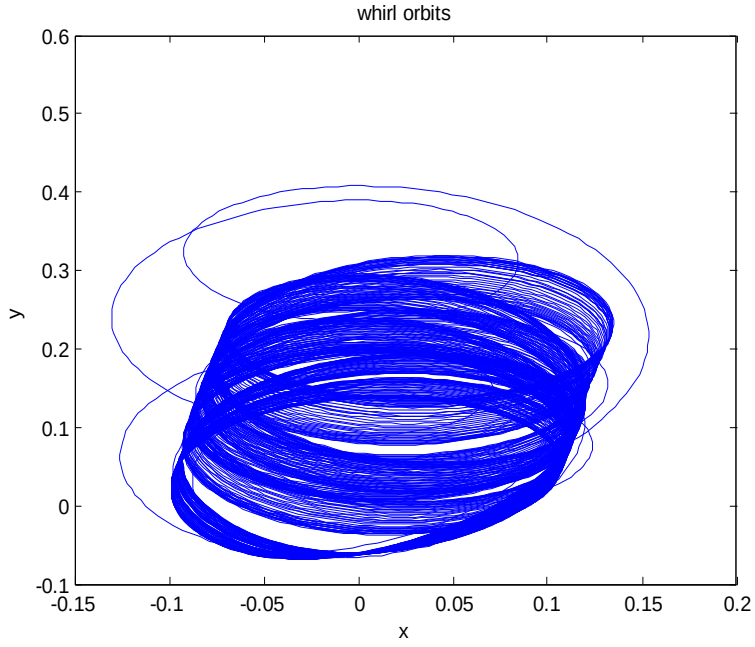

Fig 3.11 Whirl Orbit

Fig 3.12 is Poincare map for same $\Omega = 6$ .As there are more number of points which indicates that for every time period amplitude of motion is varying and hence the system is chaotic state

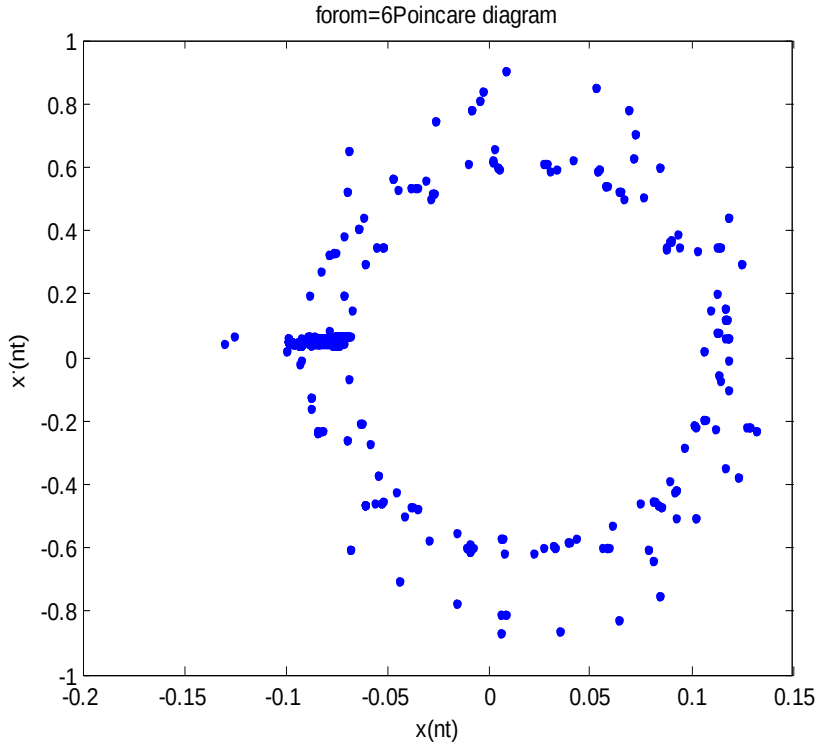

Fig 3.12 Poincare Map,

Fig 3.13 and 3.14 are time history plot for $\Omega = 5.5$ .with maximum amplitude of 0.16 and 0.4 in x and Ydirections respectively.

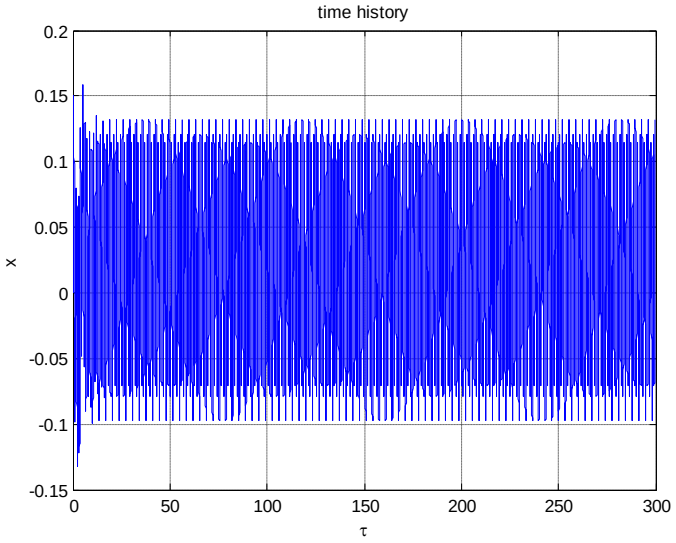

Fig 3.13 Time History

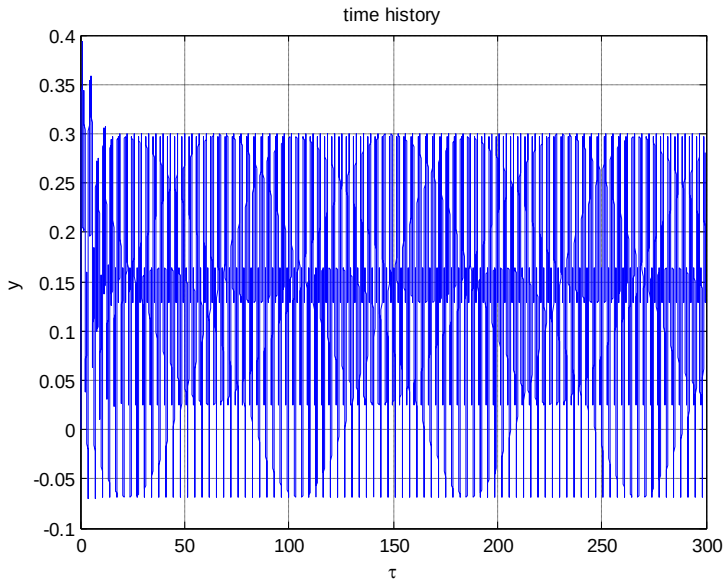

Fig 3.14 Time History

From Fig 3.15 and Fig 3.16 which are phase plane plots it can be observed that there are finite number of curves with few different centres .from this it can be inferred that the sytem to be in Quasi periodic state.

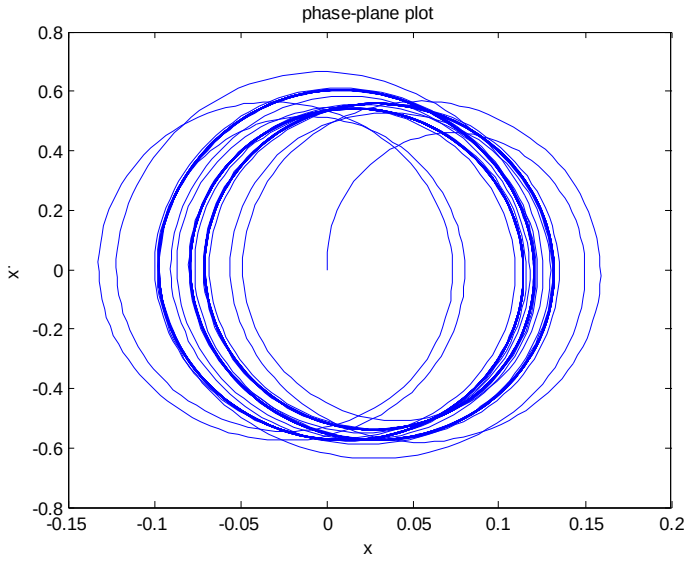

Fig 3.15 Phase Plane Plot

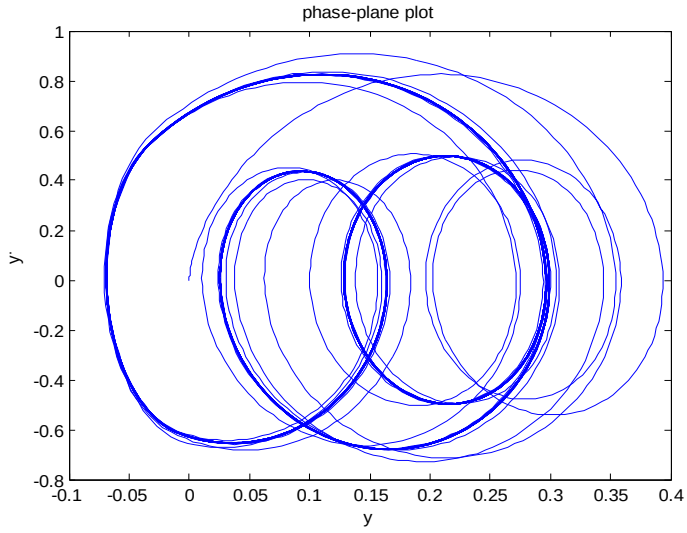

Fig 3.16 Phase Plane Plot

WHIRL ORBIT

Fig 3.17 and Fig 3.18 are whirl orbit and poincare map. As Poincare maps are forming a closed loop it can be conclude that the motion of rotor may be in quasi periodic state for $\Omega = 5.5$.

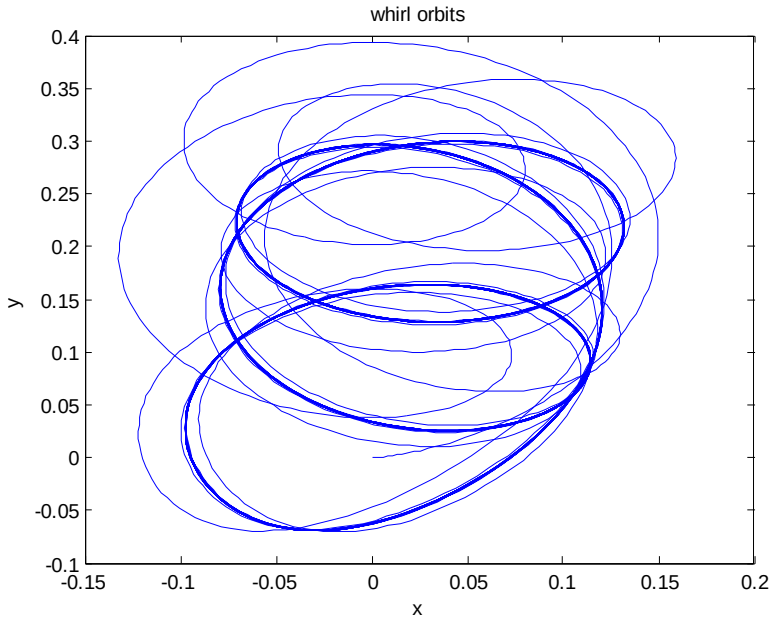

Fig 3.17 whirl Orbit

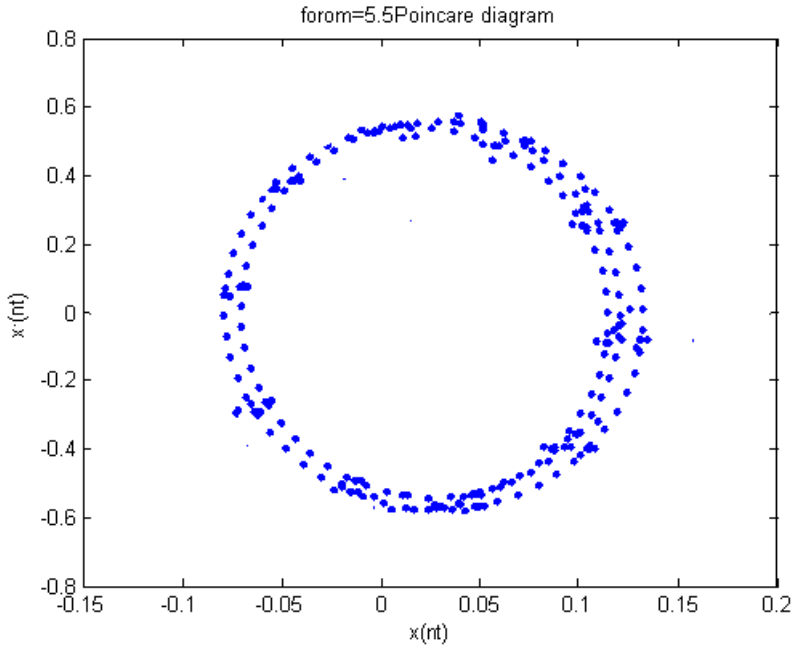

Fig 3.18 Poincare map

Graphs for U as $Variable$ for U=0.1

Fig 3.19 and 3.20 are the time history graphs for U=0.1 .for this value of U the maximum amplitude is 0.18 in X direction and 0.45 in y direction

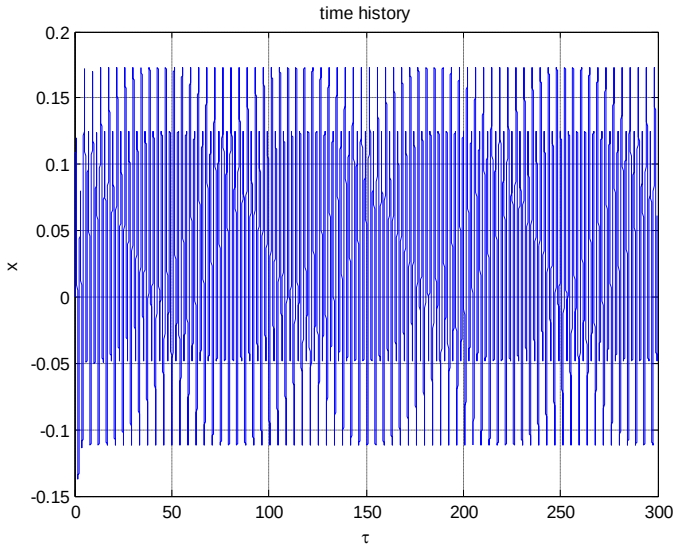

Fig 3.19 Time History

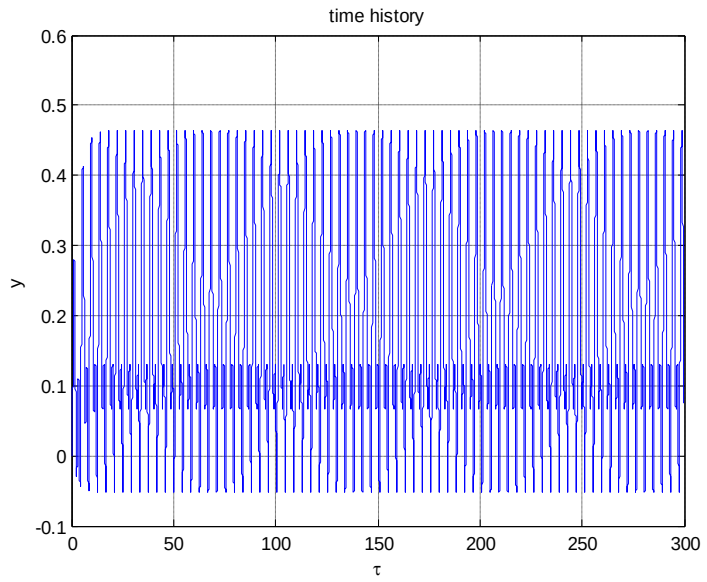

Fig 3.20 Time History

As Figures 3.21 and 3.22 which are phase plane curves for U=0.1 are simple and having finite number of curves with few centres ,the system would be in stable state.

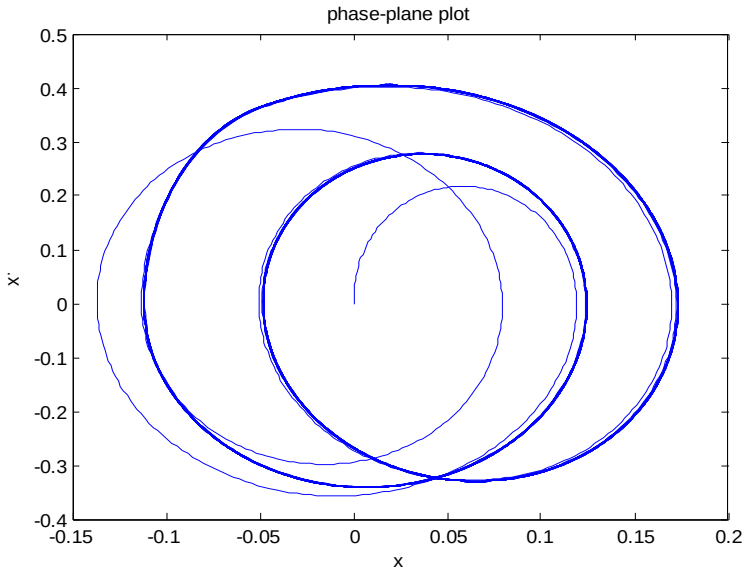

Fig3. 21

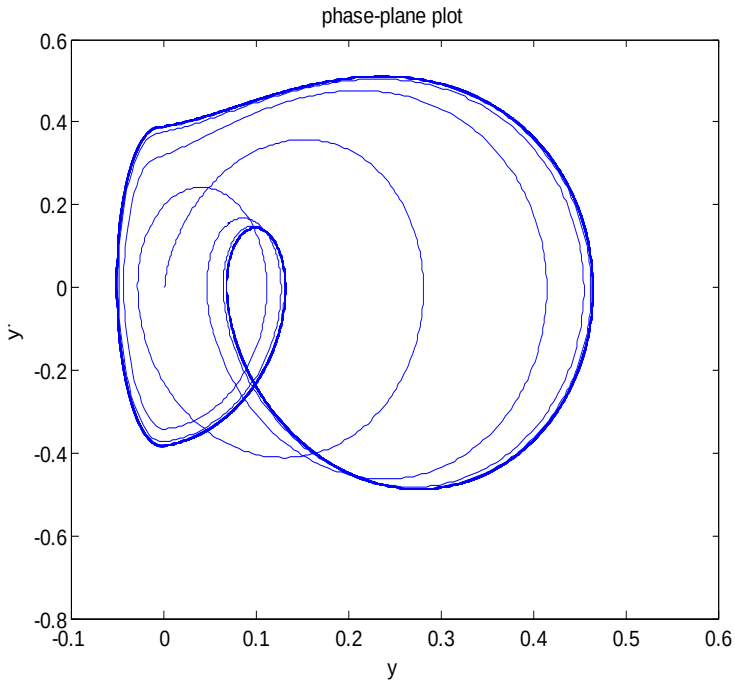

Fig 3.22 Phase Plane Plot

WHIRLORBITS

Fig 3.23 and 3.24 are whirl orbit and Poincare maps for U=0.1 respectively. As Poincare maps are finite the system will be exhibiting periodic motion

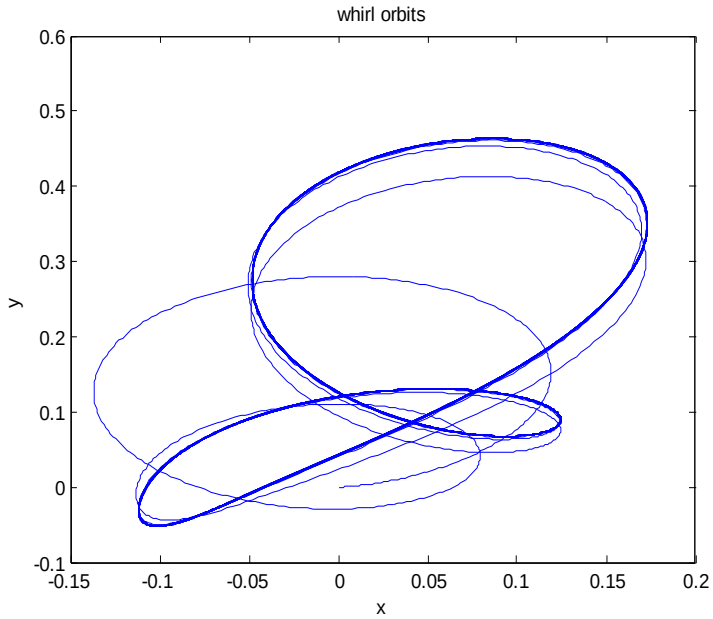

Fig 3.23 Whirl Orbit

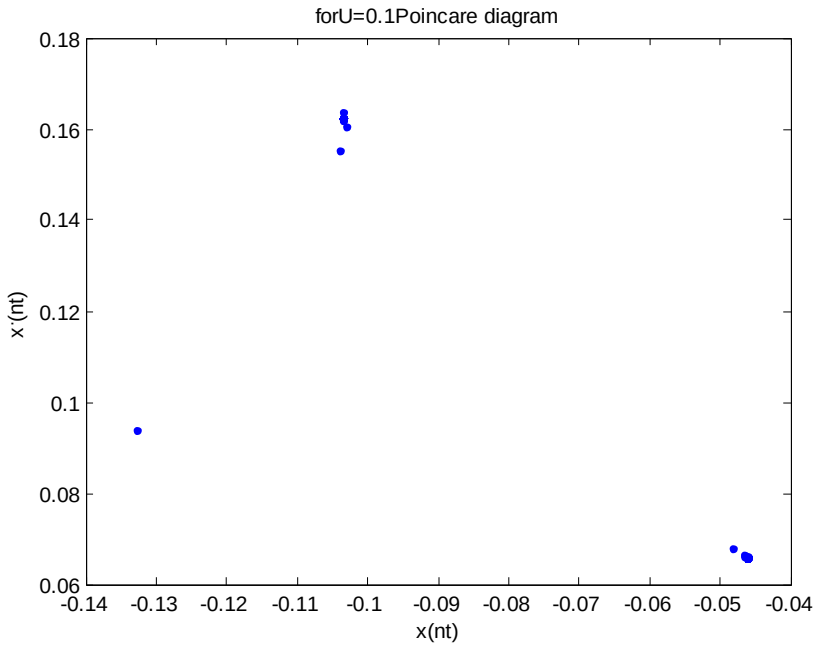

Fig 3.24 Poincare map

Graphs For U=0.5

Fig 3.25and 3.26 are amplitude plots with respect to time and reveal the unstability of the system because for every time period it can be clearly seen that the amplitude is changing.

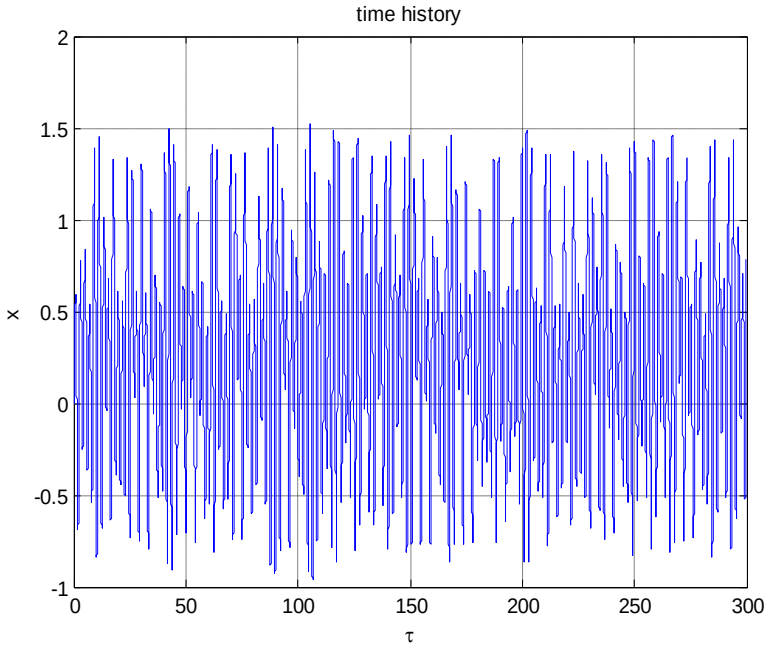

Fig 3.25 Time- History

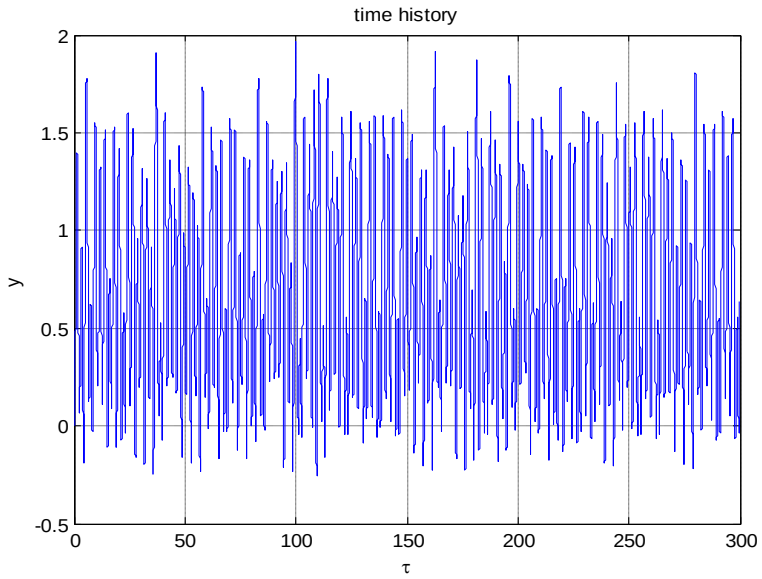

Fig 3.26 Time- History

Fig 3.27 and 3.28 are phase plane plots.In this plot it is claearly visible that the curves are so many in number and they do not have finite centres too ie., curves are complicated so we can conclude that motion would be chaotic.

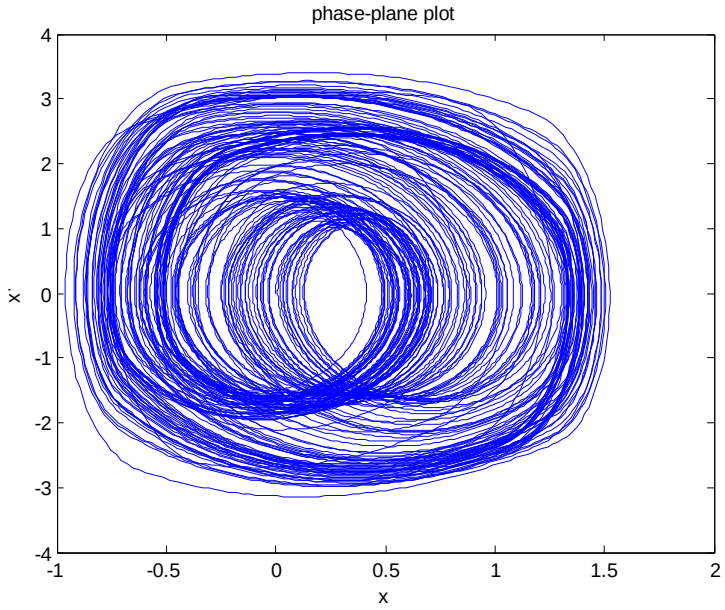

Fig 3.27 Phase Plane Plot

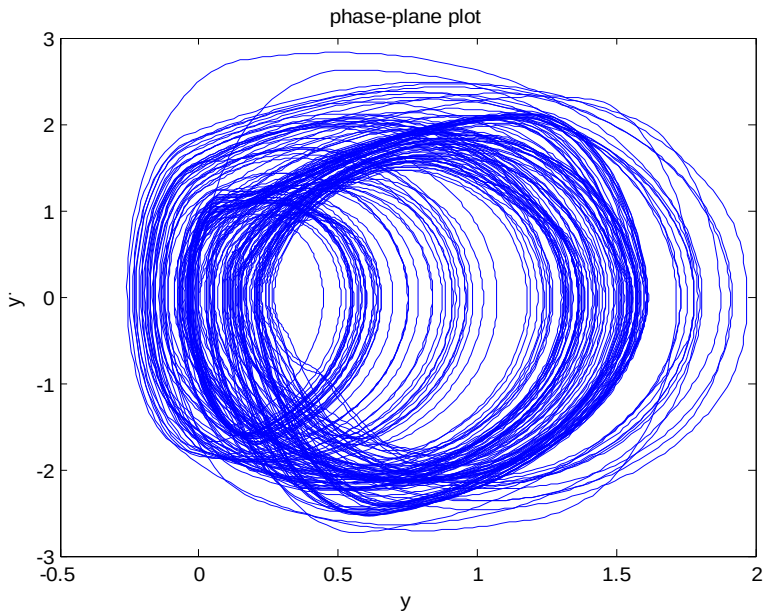

Fig 3.28 Phase Plane Plot

Fig 3.29 and Fig 3.30 are the whirl orbits and Poincare maps for U=0.5.As whirl orbit is having irregular curves with no finite centre and as Poincare maps are so many with randomly distributed the motion of rotor is chaotic

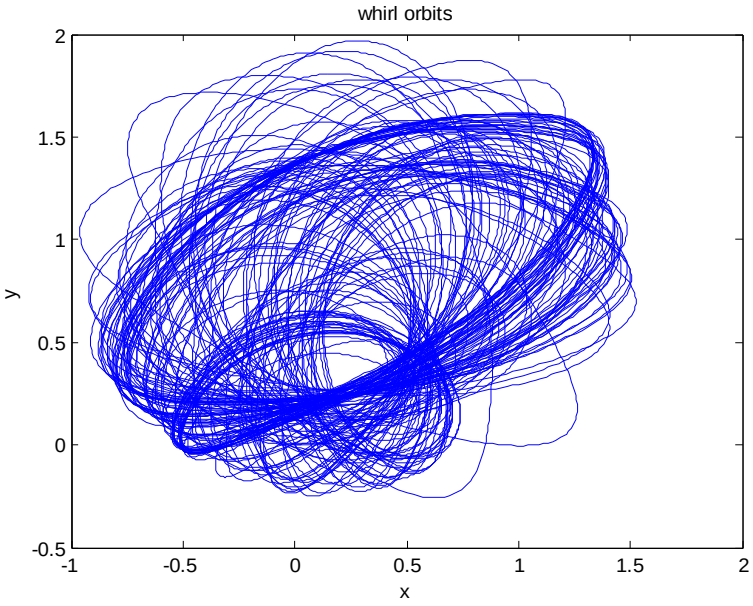

Fig 3.29 Whirl Orbit

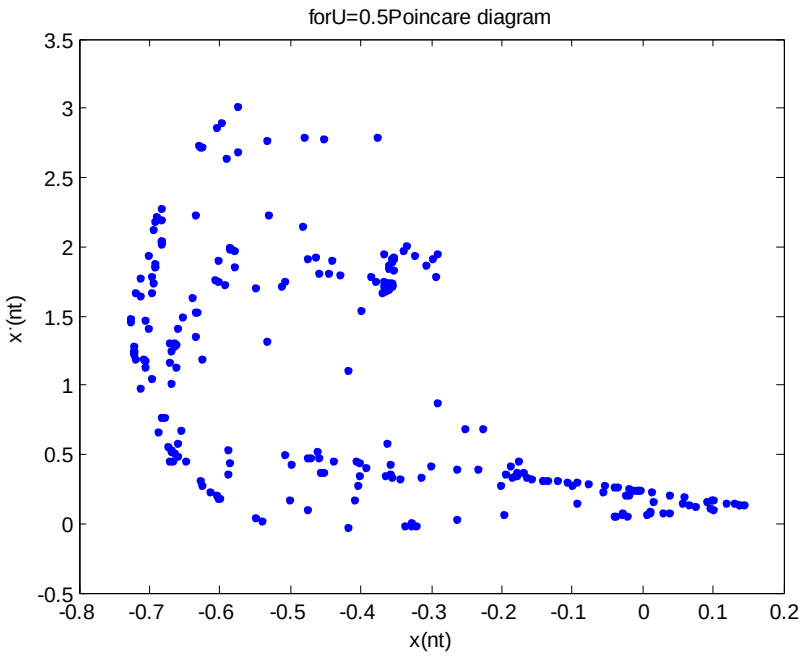

Fig 3.30 Poincare map

Fig 3.31 shows time history plots for rotor and stator when stator stiffness is considered.In these plots $X_r$and Y_r are the rotor amplitude in x and y directions and X_s and Y_s are the stator displacement in x and y direction.These plots are for values r_1 =0.95 and $r_2 = 0.01$.From these figures we can see t hat amplitude of rotor is constant and of that stator is very less and decreasing.

Fig 3.32 indicates rotors displacement for $r_2 = 0.01$ and r_1 is varied.As r_1 is varied rotor displacement is increasing at first and reached maximum and decreased

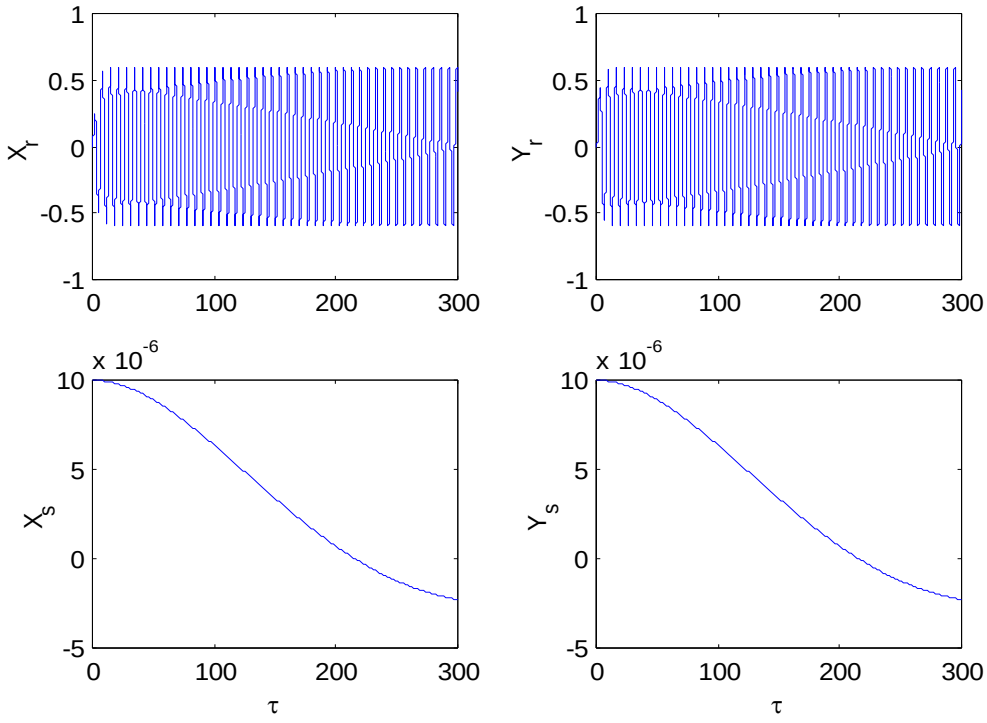

Fig 3.31

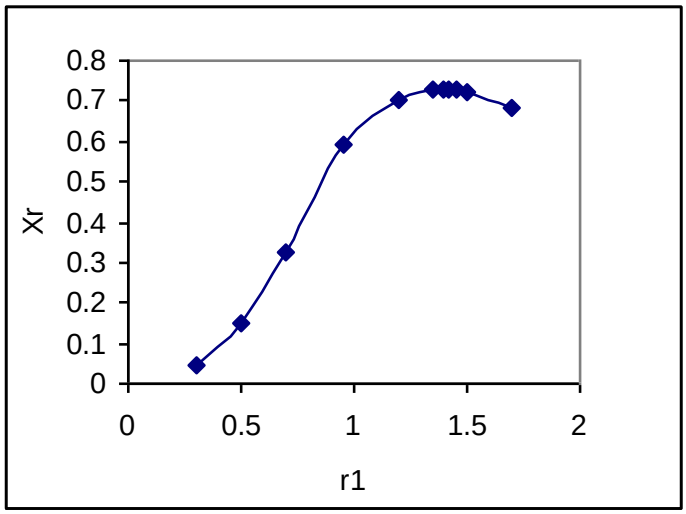

Fig 3.32

Fig 3.33 shows the difference in amplitudes for $r_2 = 0.01$ and $r_2 = 100$ when r_1 is increasing The difference in amplitudes are much larger for these two values.

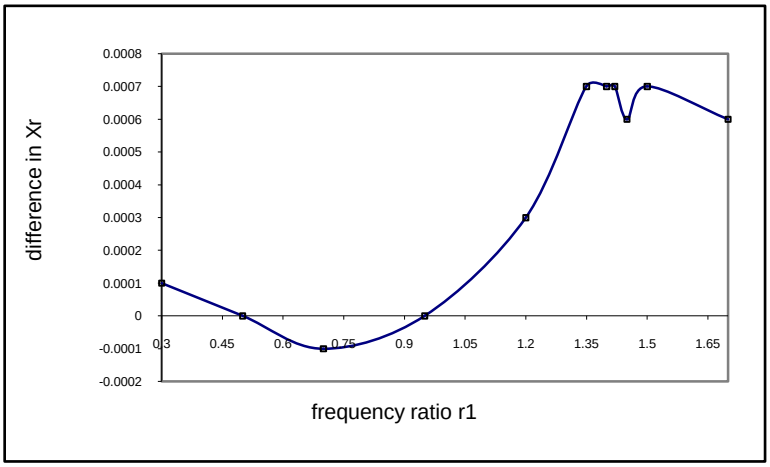

Fig 3.33

Fig 3.34 represents Frequency spectrum at r_1=1.82 and r_2=0.01 (sampling frequency=285 Hz) and broadband noise in the spectrum during earlier regions indicates a transient chaotic response

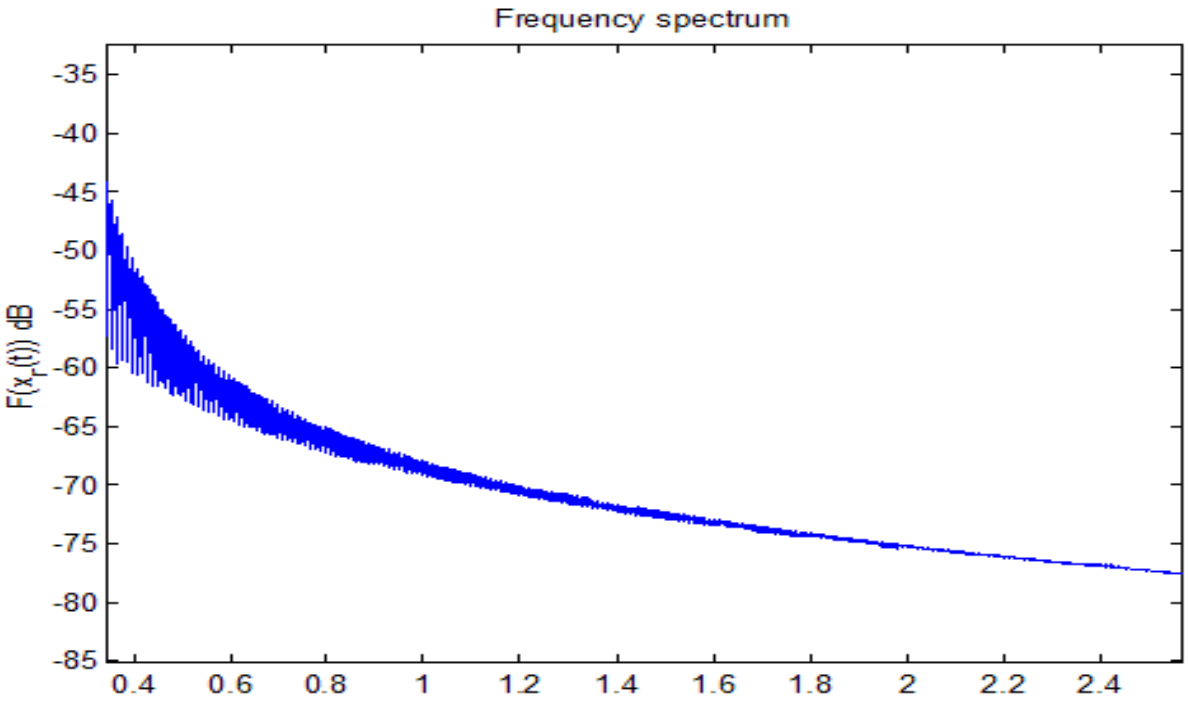

Fig 3.34 Frequency spectrum

From Fig.3.35, we can observe that is no much large difference in outputs by these two methods .But Newmarks technique is employed because it is some what faster in execution

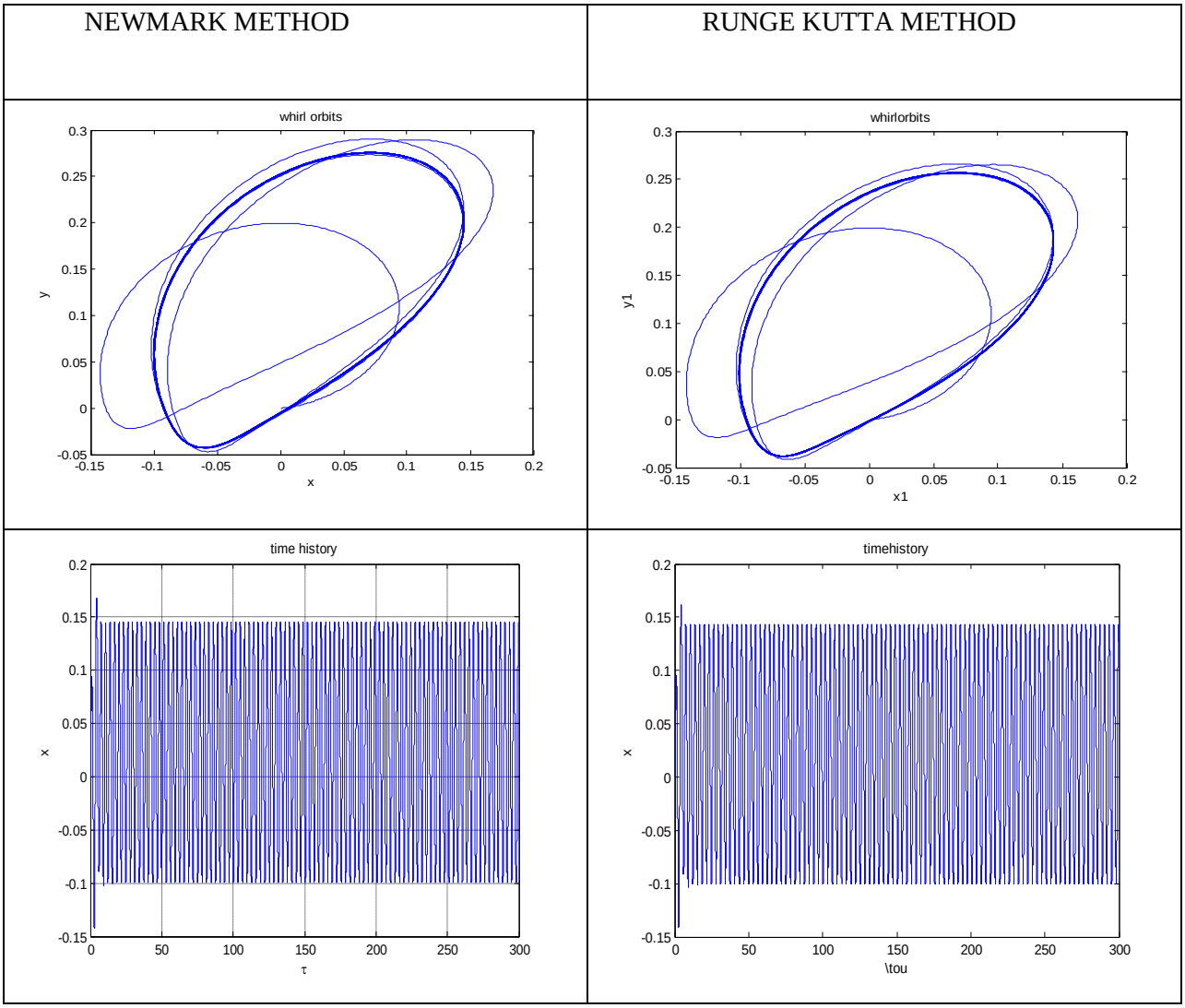

Fig 3.35

3.3 Finite Element Analysis Solution

Fig 3.36 is Campbell plot obtained from four element assembly procedure. Through this plot we can know the first three natural frequencies of rotor and variation of natural frequency with increase in speed.

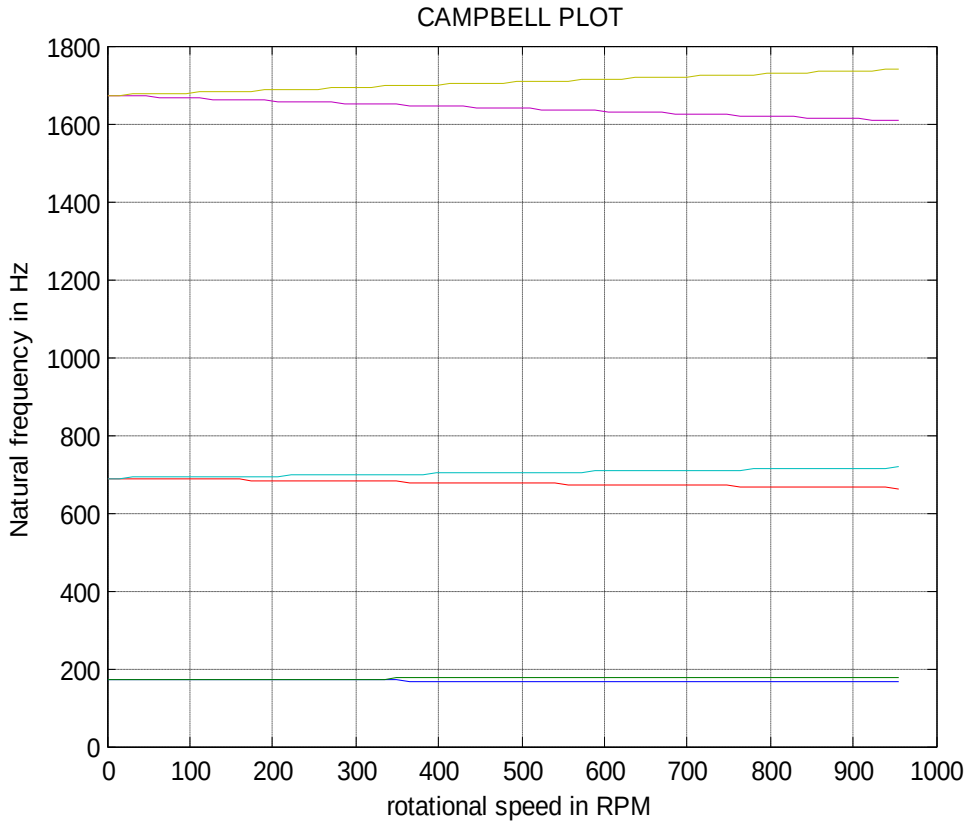

Fig 3.36

Fig.3.37 also shows the similar plot as obtained from the following ANSYS program:

```
%%%%%%%%%%%%%%%%%%%%%%%%%%%%%%%%%%%%%%%%%%%%
Lx=1000e-3
dia=50e-3
/PREP7
ET,1,16
R,1,dia,dia/2
MP,EX,1,1.97e11
MP,DENS,1,7810
MP,PRXY,1,0.3
n,1
n,10,Lx
fill,1,10
e,1,2
egen,9,1,-1
d,1,uy,,, ,,uz
d,10,uy,,, ,,uz
finish
/SOLU
antype,modal
modopt,qrdamp,5,,,on
qrdopt,on
mxpand,5,,,yes
coriolis,on,,,on
omega,0.
```

```
solve
omega,5000.
solve
finish
/POST1
plcamp
prcamp
finish
%%%%%%%%%%%%%%%%%%%%%%%%%%%%
```

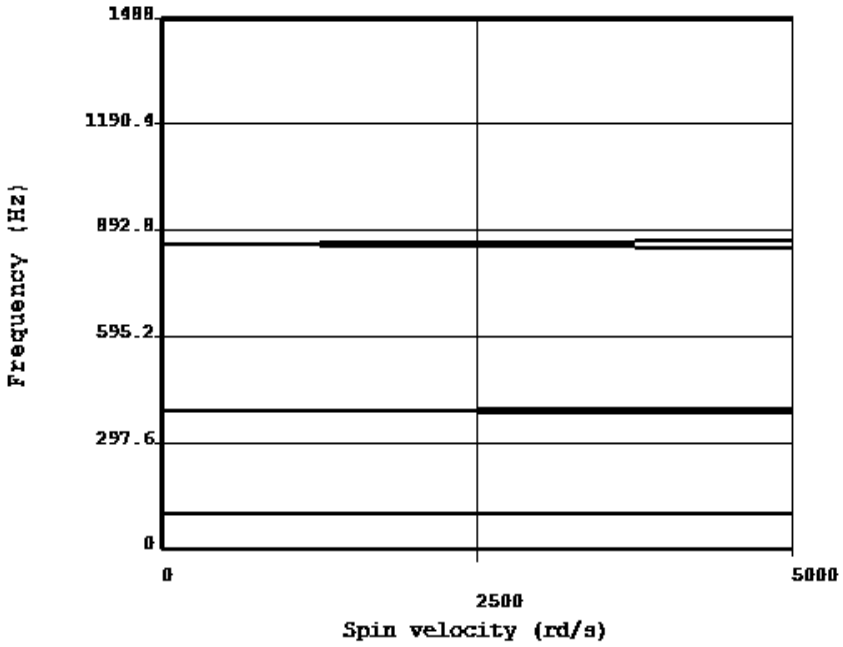

Fig.3.37 Campbell plot as obtained from 10 element approximation

Fig 3.38 shows time history of rotor for rotational speed 100rpm using Newmark solver.

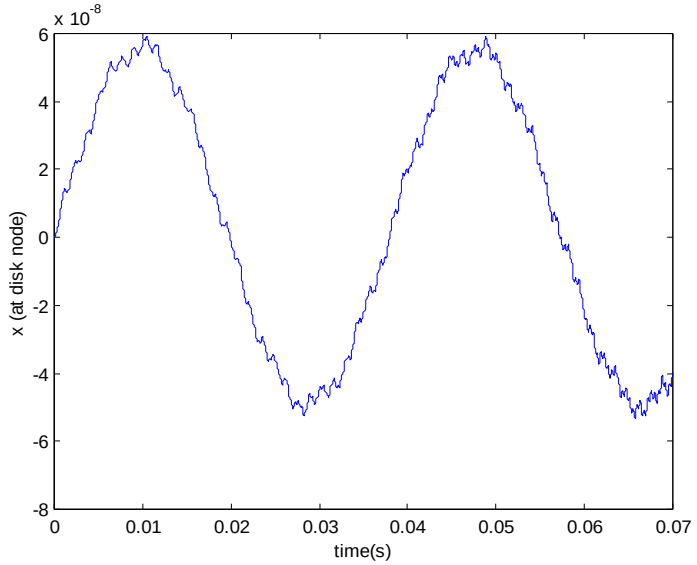

Fig3.38

Table 3.1 shows the natural frequencies of the shaft system along using our program, ANSYS result and from Euler's beam theory.

Table-3.1 Summary of Modal analysis data at standstill condition (zero speed)

Natural frequency in Hz	Matlab Timoshenko beam	Matlab Euler's beam	Theoretical $(n^2\pi^2/L^2)(EI/\rho A)^{0.5}$	ANSYS (Ten-element) outputs
BW1	172.1	197.3	98.61	98.15
FW1	172.1	197.3	98.61	98.15
BW2	689	794.6	394.44	387.45
FW2	689	794.6	394.44	387.45
BW3	1617	1879	887.49	855.13
FW3	1617	1879	887.49	855.13

It is seen that for more accuracy some more elements are still needed. Still, we need to validate the finite element program and integrate with the Newmark's solver to get the time histories and phase-trajectories at bearings and at the disk nodes.

4. CONCLUSIONS

4.1 Summary

In this work an attempt has been made to predict the rotor nonlinear instability when there is a rub-impact between rotor and stator. Three different models have been considered to model the shaft having central disk system. It was considered simply-supported boundary conditions for the shaft. Equations of motion were formulated in terms non-dimensional parameters. In first case general case of Jeffcott rotor model was selected; in second case the effect of stator flexibility on first model was added. Last model includes the four element finite element beam formulation. The equations were solved using Newmark time integration technique to obtain rotor amplitude and velocity. Outputs were shown as time histories, phase plane plots, whirl orbits and Poincare maps so as to study stability of rotor dynamic system by varying different parameters. Here in present work speed and unbalance were varied and their effect on rub impact was studied. In order to validate the results the equations were also solved by using Runge-Kutta fourth order method. After simulation, it is observed that for Ω=0.5 to2.5 system was executing periodic motion and chaotic motion of rotor was observed to be at values of speed ratio Ω=6, 7. 5, 8 and quasi periodic motion was seen at Ω=3 to 5and at 8.5,6.5,5.5,7. It is also observed that if unbalance ratio U is 0.5, the motion of rotor is chaotic and from 0.1 to 0.2, motion of rotor is periodic and from 0.3 to 0.4 motion of rotor is quasi periodic. Also it was observed that effect of stator stiffness has been very low on the overall response. Finally, the finite element modelling of rotor using four Timoshenko beam elements has been found to be less accurate in respect of modal analysis results.

4.2 Future Scope

The work presented in this thesis doesn't consider bearing dynamics which also affects the rotor dynamic stability. So, this work can be extended by considering bearing dynamics. So, this work can be extended by considering bearing dynamics. More insights of system instability have to be studied through finite element modeling and it needs verification with lumped-parameter models. In this work we considered a simple Jeffcott model in which a single disk is mounted on a shaft but in industries multi disks will be mounted in a single shaft. So in future we can also work on this multi disk model. Sometimes the diameter of shaft varies at every section .This type of model can be easily solved through finite element modelling. In present work, forces due to gas or fluid acting on disk blade were not considered which is a situation in gas turbines or steam turbines etc. So by including this type of forces we can work in future.

REFERENCES

1. R.F.Beatty, Differentiating Rotor response due to radial rubbing, *Journal of Vibration, Acoustics, Stress ,and Reliability in Design* Vol107 pp151–160, 1985.
2. F.K.Choy and J.Padovan,Non-linear transient analysis of rotor-casing rub events, *Journal of Sound and Vibration* Vol 113 pp 529–545, 1987.
3. Y.S.Choi and S.T.Noah, Nonlinear steady-state response of a rotor support system, *Journal of Vibration , Acoustics ,Stress ,and Reliability in Design* Vol 109 pp255–261,1987.
4. F.Chu and Z.Zhang, Bifurcation and chaos in a rub impact Jeffcott rotor system, *Journal ofSoundandVibration*, Vol 210, pp 1–8, 1998.
5. S.Edwards,A.W.Lees and M.I.Friswell,The influence of torsion on rotor/stator contact in rotating machinery, *Journal of Sound and Vibration* Vol225 pp767–778, 1999.
6. Z.Shang ,J.Jiang and L.Hong, The global responses characteristics of a rotor/stator rubbing system with dry friction effects, *Journal of Sound and Vibration* doi:10.1016/j.jsv.2010.06.004
7. S. Roques , M.Legrand , P.Cartraud , C.Stoisser and C.Pierre 'Modeling of a rotor speed transient response with radial rubbing, *Journal of Sound and Vibration* Vol 329 pp527–546,2010.
8. Q.-S. Lu Q.-H. Li and E.H.Twizell, The existence of periodic motions in rub-impact rotor systems, *Journal of Sound and Vibration* Vol 264 pp1127–1137 ,2003.
9. X.Shen, J.Jia and M.Zhao, Nonlinear analysis of a rub-impact rotor-bearing system with initial permanent rotor bow, *Arch Appl Mech*, Vol. 78, pp.225–240,2008.
10. J.D. Jeng , YuanKang and Yeon-PunChang, An alternative Poincare´ section for high-order harmonic and chaotic responses of a rubbing rotor, *Journal of Sound and Vibration*, Vol. 328 pp 191–202, 2009.
11. S. Ziaei-Rad , E.Kouchaki and M Imregun, Thermoelastic Modeling of Rotor Response With Shaft Rub, *Journal of Applied Mechanics* Vol. 772 DOI: 10.1115/1.4000904 ,2010.
12. F. Chu and W.Lu, Determination of the rubbing location ina multi-disk rotor system by means of dynamic stiffness identification, *Journal of Sound and vibration*, Vol. 248(2), pp235-246, 2001.
13. C.Fulei and Z.Zhang, Periodic,Quasi periodic,and Chaotic vibrations of a rub Impact rotor system supported on oil-film Bearings, *Int.J.Engg.Science*, Vol 35 pp 963-973,1997.
14. F. Chu, Stability and non-linear responses of arotor-bearing system with pedestal looseness, *Journal of sound and vibration* vol 241(5), pp 879-893, 2001.
15. Z.K. Penga, F.L. Chua and P.W. Tseb, Detection of the rubbing-caused impacts for rotor–stator fault diagnosis using reassigned scalogram, *Mechanical systems and signal processing*, *V*ol.19 pp 391–409 2005.

16. Y.B. Kim and S.T. Naoh, Bifurcation analysis for modified Jeffcott rotor with bearing clearances, *Nonlinear Dynamics* Vol. 1 pp 221-241,1990.
17. H. Diken, Non-linear vibration analysis and subharmonic whirl frequencies of the Jeffcott rotor model, *Journal of Sound and vibration*, Vol. 243(1), pp117-125, 2001.
18. Y .B. Kim, S.T. Noah and Y. S. Choi, Periodic response of multi-disk rotors with bearing clearances, *Journal of Sound and Vibration* Vol.144(3) pp381-395, 1991.
19. T.H.Patel and A.K.Darpe, Coupled bending torsional vibration analysis of rotor with rub and crack, *Journal of Sound and Vibration* Vol.326 pp 740–752 2009.
20. C.W.Chang-jian and C.K.Chen , Chaos and bifurcation of a flexible rub-impact rotor supported by oil film bearings with nonlinear suspension, *Mechanism and Machine Theory* Vol.42 pp 312–333 2007.
21. X.Shen, J.Jia and M.Zhao, Effect of parameters on the rubbing condition of an unbalanced rotor system with initial permanent deflection, *Arch Appl Mech* Vol.77, pp 883–892, 2007.
22. P. Pennacchi and A.Vania, 'Analysis of Rotor-to-Stator Rub in a Large Steam Turbogenerator,' *International Journal of Rotating Machinery* doi:10.1155/2007/90631.
23. F. Chu,and W.Lu, Stiffening effect of the rotor during the rotor-to-stator rub in a rotating machine, *Journal of Sound and Vibration* Vol.308 pp 758–766 2007.
24. F.Chu and W.Lu, Experimental Observation of Nonlinear vibrations in a rub impact rotor system, *Journal Of sound and Vibration*,Vol-283,pp.621-643,2005.
25. M.A.Abuziad,M.E.Eleshaky and M.G.Zedan, Effect of partial rotor- to- stator rub on shaft vibration, *J. Mechanical Science and Technology*,Vol-23,pp 170-182,2009
26. W.M.Zhang and G.Meng, Stability, bifurcation and chaos of a high speed rub impact rotor system in MEMS, *Sensors and Actuators*,A,Vol.127,pp163-178 2006.
27. W.Li, Y.Yang, D.sheng and J.Chen, A novel nonlinear model of rotor/bearing seal system and numerical analysis, *Mechanism and Machine Theory*, pp.618-631,2011.
28. Y.Yang, S.Zhang, Q.han and Y.Qu, Characteristics of variable parameters in rotor system with rub impact fault, *Proc.8thworld congress on International amd Automation*, July 6-9, 2010, Jinan,chinqa, pp.5947-5952.
29. J.Zapomel and P.Ferfecki, A Computational investigation of the disk-housing impacts of accelerating rotors Supported by hydrodynamic bearings, *J.Applied Mechanics, Trans.ASME*, Vol.78, p.021001-1, 2010.
30. T.H.Patel and A.K.Darpe, Study of coast-up vibration response for rub detection, *Mechanisms and Machine Theory*, Vol.44, pp.1570-1579, 2009.